THE UNIVERSITY OF SYDNEY

AMME3500

Assignment 3

S.J. Tan

311225659

29 May 2016

List of Figures

Contents

1 Bode Plots and State Space

1.1 Bode Plots and Frequency Response

(a) Bode Plots

i. Proportional Controller

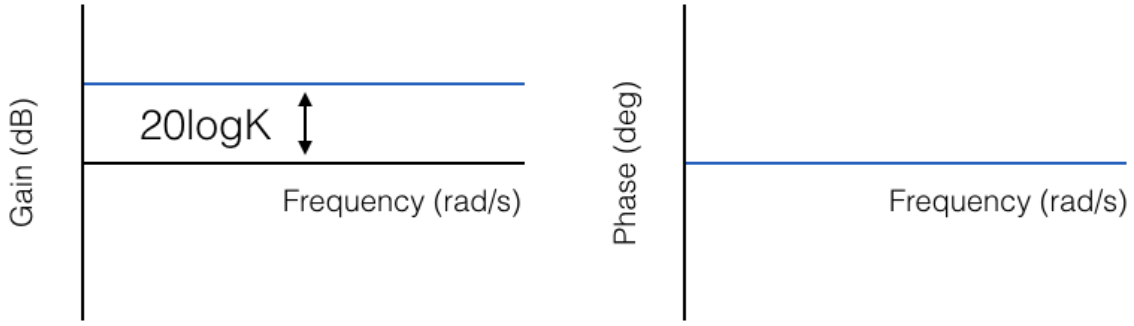

Figure 1: Bode plots for a proportional controller.

For proportional control $G(s) = K$, the gain curve is a constant at $20\log K$ dB while the phase is zero (Fig. 1). This acts simply to scale the system response and does not affect its phase. This is evident in an example shown in Fig. 2, where the system with positive gain has the same phase but an amplified magnitude. By amplifying the magnitude, the phase margin is also increased. Therefore, proportional controllers can be used to design for percentage overshoot. The relationship between damping ratio and phase margin exists:

$$\Phi_M = \tan^{-1} \frac{2\zeta}{\sqrt{-2\zeta^2 + \sqrt{1 + 4\zeta^4}}} \tag{1}$$

To design for % OS, convert the desired % OS to a damping ratio then a phase margin, and find the frequency on the phase diagram that yields the desired phase margin. Change the gain by the necessary amount to lift or lower the magnitude curve, essentially forcing it to produce the desired phase margin [1].

In general, the benefits of proportional control can be a faster transient response and improved steady-state error. As seen in the loop-shaping method, gain can be tailored to meet the desired phase margin, which controls overshoot, and concurrently, stability.

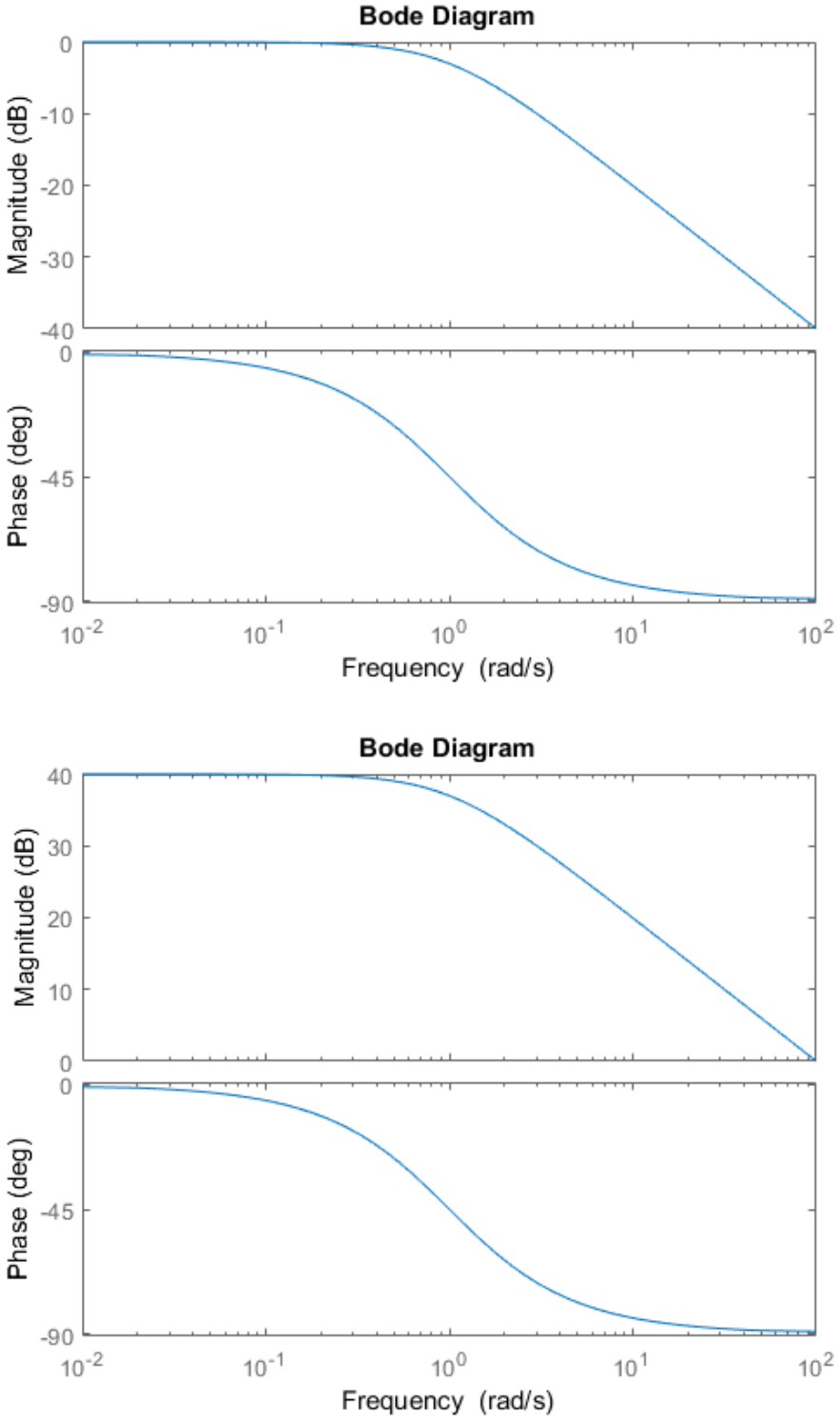

Figure 2: Top: $G(s) = 1/(s+1)$. Bottom: $G(s) = 100/(s+1)$

ii. PI Controller

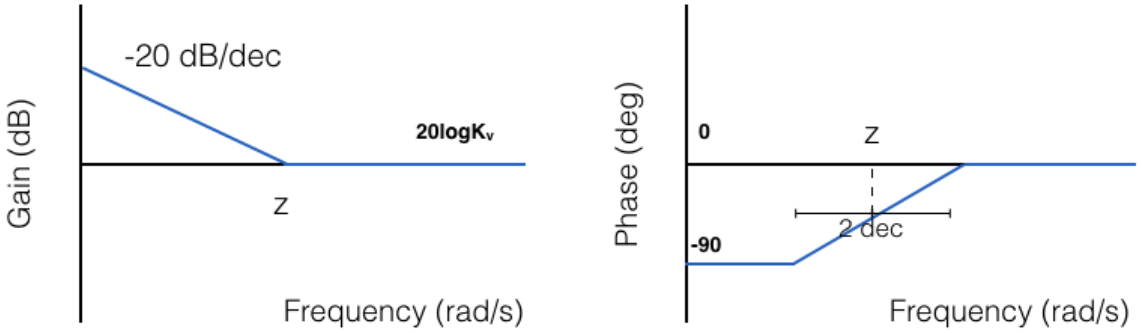

Figure 3: Gain and phase plots for $G(s) = K(s+z)/s$.

While a PI controller is typically given as $G_O(s) = K_p + K_i/s$, the terms must be combined to have a common denominator of s to sketch the controller as a single Bode plot so that $G(s) = K(s+z)/s$, where K and z are some function of K_i and K_p.

The gain curve shows high gain at low frequencies and constant gain at frequencies higher than that of the zero. The phase curve begins at -90 degrees and rises at 45 deg/dec beginning one decade before the frequency of the zero and ending one decade after.

The gain is infinitely high at low frequencies, which desirably eliminates steady-state error. However, a decrease in phase also occurs at low frequencies. This can diminish the phase margin, which can increase the overshoot or make the system less stable. For this reason, it is usually advised that the break frequency be placed substantially lower than the crossover frequency to minimise the effect on phase margin [1].

iii. Lead

For $G(s) = K(s+z)/(s+p)$ where $z < p$, the gain plot starts at $20\log K_v$ where K_v is the DC gain, obtained from expressing $G(s)$ in standard form. At the frequency of the zero, the gain increases 20 dB/dec, then becomes constant at the frequency of the pole due its equal magnitude but opposite sign contribution.

The lead compensator adds phase lead. Its phase begins at 0 degrees then increases by 45 deg/dec beginning one decade before the location of the zero and ending one decade after. The phase is then constant until it is affected by the pole, decreasing by 45 deg/dec beginning one decade before and ending one decade after.

The lead compensator increases the system's bandwidth by increasing the gain crossover frequency (provided the crossover occurs after the frequency of the zero).

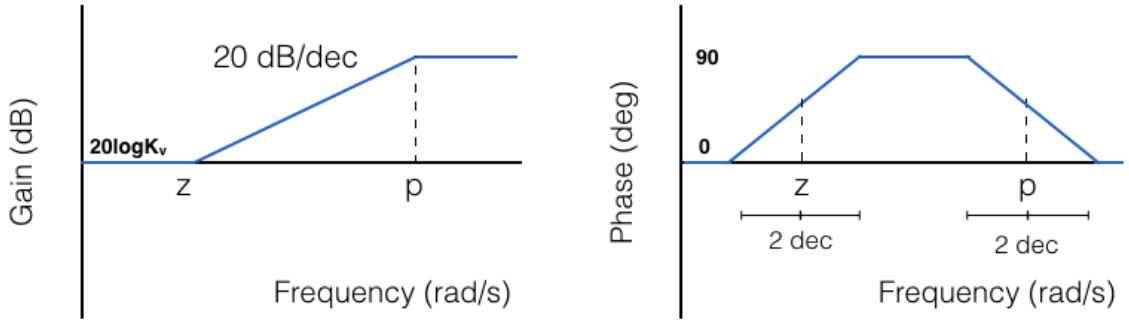

Figure 4: Gain and phase plots for $K(s+z)/(s+p)$; $z < p$.

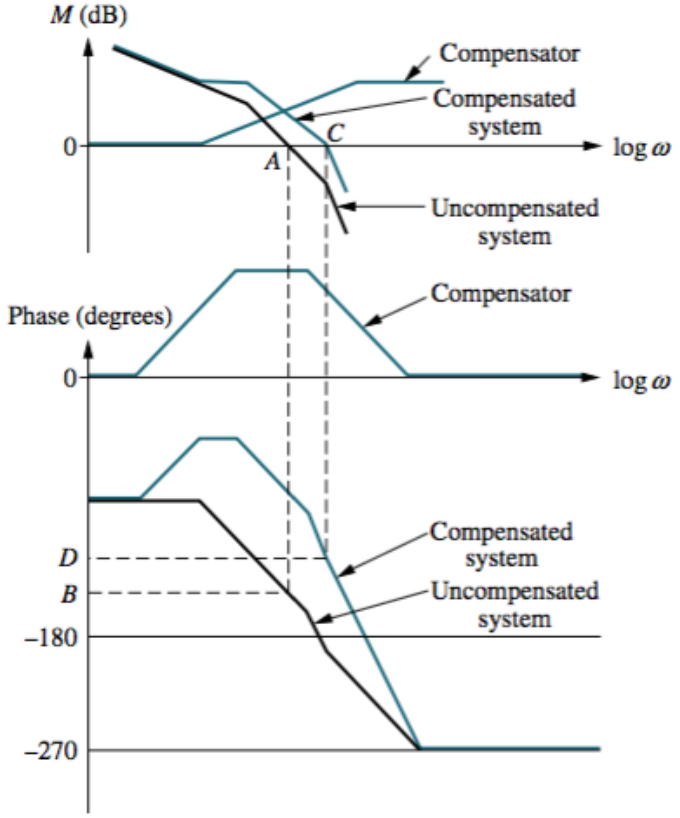

Figure 5: Visualising lead compensation [1].

Because the gain crossover frequency is increased, a faster transient response is realised. Additionally, the phase margin is also increased (Fig. 5). This acts to reduce the percentage overshoot, apparent in the phase margin-damping ratio relation (Eq. 1).

Note, however, that if the original system's gain margin is quite close to zero, care should be taken so that the lead controller does not make the system unstable by raising system gain towards or above 0 dB.

Because the initial magnitude is constant, the steady-state error is not affected by the addition of a lead controller.

iv. Lag

The lag compensator of $G(s) = K(s + z)/(s + p)$ where $p > z$ decreases the gain at higher frequencies and adds phase lag. The gain curve begins again at $20\log K_v$ but decreases beginning the frequency at the zero, then is constant once meeting the frequency at the pole. The phase curve starts at 0 degrees, then tends to -90 degrees from the zero contribution and rises back up to 0 degrees with the pole contribution.

The lag compensator can stabilise a system while maintaining a high gain, which improves the steady-state error. For example, Fig. 7 shows an original system with a high K_v that is unstable because the gain is higher than 0 dB at 180 degrees phase. The lag compensator can maintain the same system gain at low frequencies, however, stabilises the system by reducing gain at high frequencies, including the crossover frequency. Nevertheless, because the crossover frequency is reduced, the response is also slower.

The lag controller will also inevitable affect the phase margin, so this can be strategically designed for to meet the system's transient response aims.

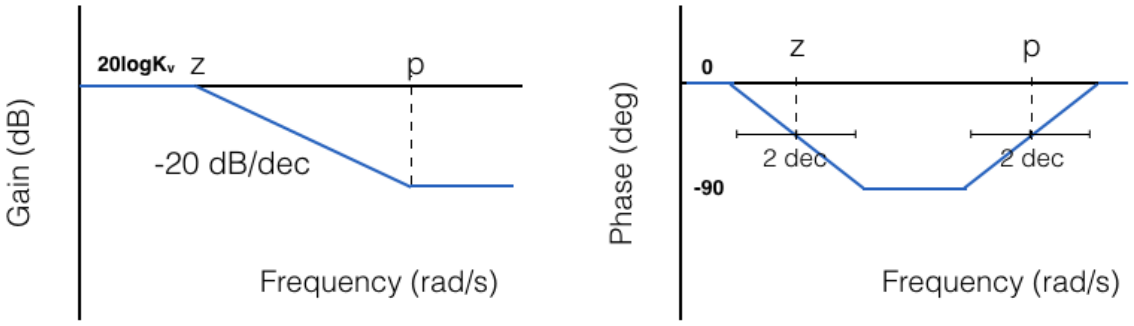

Figure 6: Gain and phase plots for $K(s+z)/(s+p)$; $p > z$.

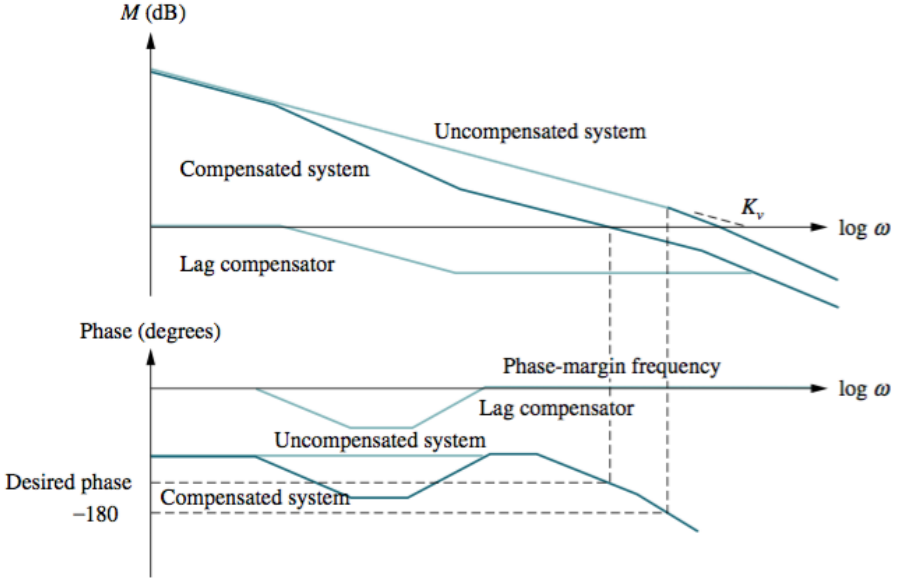

Figure 7: Visualising lag compensation [1].

(b) Loop-Shaping Method

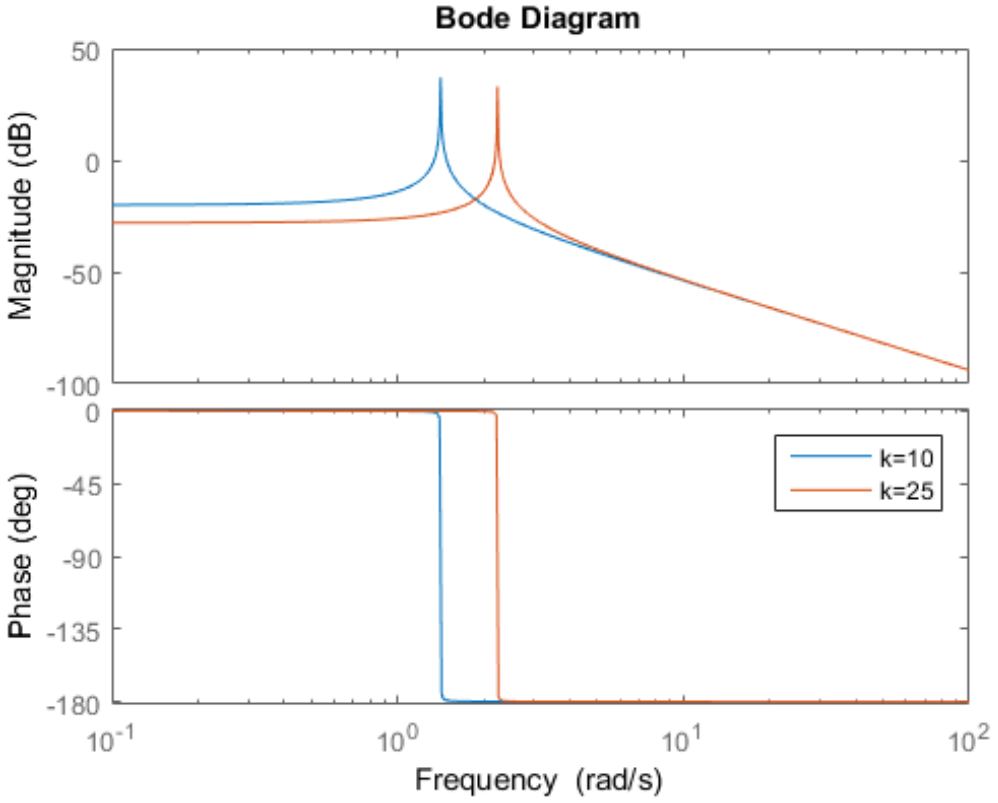

Figure 8: Open-loop Bode plots for $k = 10$ and $k = 25$.

The Bode plot for the system is shown in Fig. 8. At low frequencies, the response follows the input well in terms of phase, but is attenuated in some proportion to the k value. At the resonant frequency, the phase drops immediately to lag 180 degrees behind the input. At high frequencies, the amplitude of the oscillatory response becomes severely diminished in comparison to the input. Comparing the systems of $k = 10$ and $k = 25$, it is evident that the difference is that the system with higher k has a slightly diminished low-frequency magnitude and a later resonant peak.

Applying the loop-shaping method will be very difficult. Without knowing the exact position of the resonant peak, it will not be able to be cancelled via loop shaping. Attempting to cancel the peak without knowing its position could result not only in the peak not being cancelled, but also in further convoluting the system.

1.2 State Space

(a) Transfer Function to Phase-Variable Representation

i.

For system:

$$G(s) = \frac{4}{(s^2 + 3s + 12)} = \frac{C(s)}{R(s)} \tag{2}$$

$$(s^2 + 3 + 12)C(s) = 4R(s) \tag{3}$$

The following can be expressed, assuming zero initial conditions:

$$\ddot{c} + 3\dot{c} + 12c = 4r \tag{4}$$

The state space matrices are then:

$$\begin{bmatrix} \dot{c} \\ \ddot{c} \end{bmatrix} = \begin{bmatrix} 0 & 1 \\ -12 & -3 \end{bmatrix} \begin{bmatrix} c \\ \dot{c} \end{bmatrix} + \begin{bmatrix} 0 \\ 4 \end{bmatrix} r \tag{5}$$

$$y = \begin{bmatrix} 1 & 0 \end{bmatrix} \begin{bmatrix} c \\ \dot{c} \end{bmatrix} \tag{6}$$

ii.

For the next system:

$$G(s) = \frac{20(s^2 + 3s + 2)}{(s + 4)(s^2 + 10s + 500)} = \frac{C(s)}{R(s)} \tag{7}$$

Represent it in two parts, so that the first takes the denominator:

$$\frac{X(s)}{R(s)} = \frac{1}{s^3 + 14s + 540s + 2000} \tag{8}$$

$$\dddot{x} + 14\ddot{x} + 540\dot{x} + 2000x = r \tag{9}$$

The second takes the numerator:

$$\frac{C(s)}{X(s)} = 20(s^2 + 3s + 2) \tag{10}$$

$$c = 20(\ddot{x} + 3\dot{x} + 2x) \tag{11}$$

Then the phase-variable representation becomes:

$$\begin{bmatrix} \dot{x} \\ \ddot{x} \\ \dddot{x} \end{bmatrix} = \begin{bmatrix} 0 & 1 & 0 \\ 0 & 0 & 1 \\ -2000 & -540 & -14 \end{bmatrix} \begin{bmatrix} x \\ \dot{x} \\ \ddot{x} \end{bmatrix} + \begin{bmatrix} 0 \\ 0 \\ 1 \end{bmatrix} r \tag{12}$$

$$y = c = \begin{bmatrix} 40 & 60 & 20 \end{bmatrix} \begin{bmatrix} x \\ \dot{x} \\ \ddot{x} \end{bmatrix} \tag{13}$$

(b) Controllability & Observability

i.

For the system:

$$\dot{x} = \begin{bmatrix} 0 & 1 \\ -1 & -1.5 \end{bmatrix} x + \begin{bmatrix} 0 \\ 0.25 \end{bmatrix} u, y = \begin{bmatrix} 0 & 1 \end{bmatrix} x \tag{14}$$

The controllability matrix is:

$$C_M = \begin{bmatrix} B & AB & A^2B \end{bmatrix} = \begin{bmatrix} 0 & 0.25 \\ 0.25 & -3.75 \end{bmatrix} \tag{15}$$

Its determinant is -0.625, which is non-zero, meaning the matrix is nonsingular and the system is controllable. This means that the control signal is able to control the behaviour of each state variable by strategic placement of poles.

The observability matrix is:

$$O_M = \begin{bmatrix} C \\ CA \end{bmatrix} = \begin{bmatrix} 0 & 1 \\ -1 & -1.5 \end{bmatrix} \tag{16}$$

Its determinant is 1, which means the matrix full rank. Therefore, the system is observable. This means that an observer can be designed via pole placement which allows evaluation of all state variables at the output.

ii.

For the system:

$$\dot{x} = \begin{bmatrix} 0 & 1 \\ 0 & 0.5 \end{bmatrix} x + \begin{bmatrix} 2 \\ 0 \end{bmatrix} u, y = \begin{bmatrix} 1 & 0 \end{bmatrix} x \tag{17}$$

The controllability matrix is:

$$C_M = \begin{bmatrix} B & AB & A^2B \end{bmatrix} = \begin{bmatrix} 2 & 0 \\ 0 & -0 \end{bmatrix} \tag{18}$$

Its determinant is 0, therefore, the system is not controllable. The control signal has no influence over at least one of the state variables via pole placement.

The observability matrix is:

$$O_M = \begin{bmatrix} C \\ CA \end{bmatrix} = \begin{bmatrix} 1 & 0 \\ 0 & 0 \end{bmatrix} \tag{19}$$

Its determinant is 0, which means the system is not observable. An observer can not be created that can evaluate at least one of the state variables at the output.

2 Satellite Control

2.1 Single Axis Control of a Small Spherical Satellite

(a) $\theta_s(s)/V(s)$

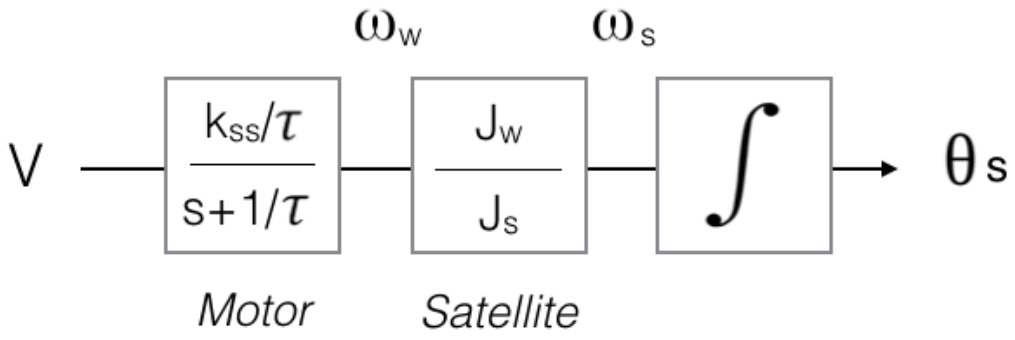

Figure 9: Block diagram of satellite system.

The block diagram of the satellite system is given in Figure 9, where specifications are given as:

- $k_{ss} = 20$ rad/V
- $J_w = 0.0520$ kg m^2
- $\tau = 0.52$ s
- $J_s = 0.4352$ kg m^2

The transfer function between applied voltage V to angular displacement of the satellite θ_s is therefore:

$$\frac{\theta_s(s)}{V(s)} = \frac{\omega_w(s)}{V(s)} \times \frac{\omega_s(s)}{\omega_w(s)} \times \frac{\theta_s(s)}{\omega_s(s)} = \frac{(J_w/J_s)(k_{ss}/\tau)}{s^2 + (1/\tau)s} \tag{20}$$

(b) Controller Design via Frequency Response

The system is simple 2nd order. Frequency response methods will be investigated. First, gain adjustment was trialled. Following a procedure outlined in Nise [1], the step response shown in Fig. 10 was achieved with 5% OS. By gain adjustment, overshoot and settling time can not be specified independently. Interestingly, the uncompensated system had a slightly faster settling time but was initially oscillatory (high overshoot). The effect of gain adjustment decreased the crossover frequency,

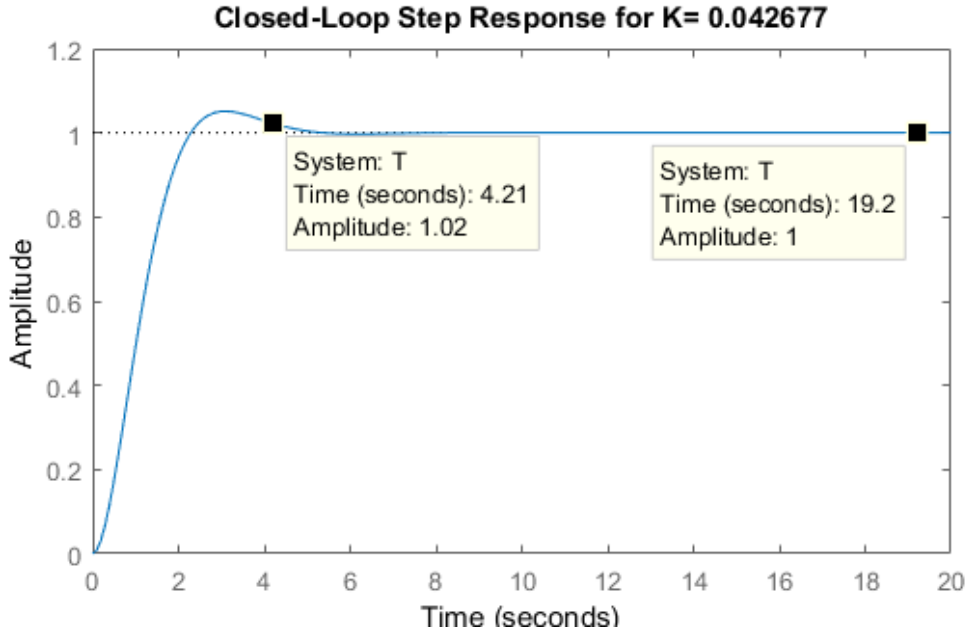

Figure 10: System via gain adjustment meets 5% OS, has zero steady-state error, but does not meet the settling time requirement.

making the system slightly slower, but increased the phase margin, which stabilised the step response. These are available in Appendix A.

It was interesting to note that the system also exhibited zero steady-state error. This is attributed to the integrator in the forward path that had already been placed to convert ω_s to θ_s. While a lag compensator was trialled, it did not really act to improve the system response as there was no error to eliminate. It achieved 5% OS but the settling time was 646 seconds (Fig 11). The procedure also follows Nise and can be ascertained from `Q2_1.m`.

Next, a lead compensator was trialled, which typically allows independent specification of settling time and overshoot. The full procedure for lead controller design is given here, where its general form is:

$$G_c(s) = \frac{1}{\beta}\frac{s + (1/T)}{s + (1/\beta T)} \tag{21}$$

1. Enumerate a DC gain K_v to meet a steady-state error requirement. The steady-state error requirement has already been met, so set K_v arbitrarily to 20V to begin with.

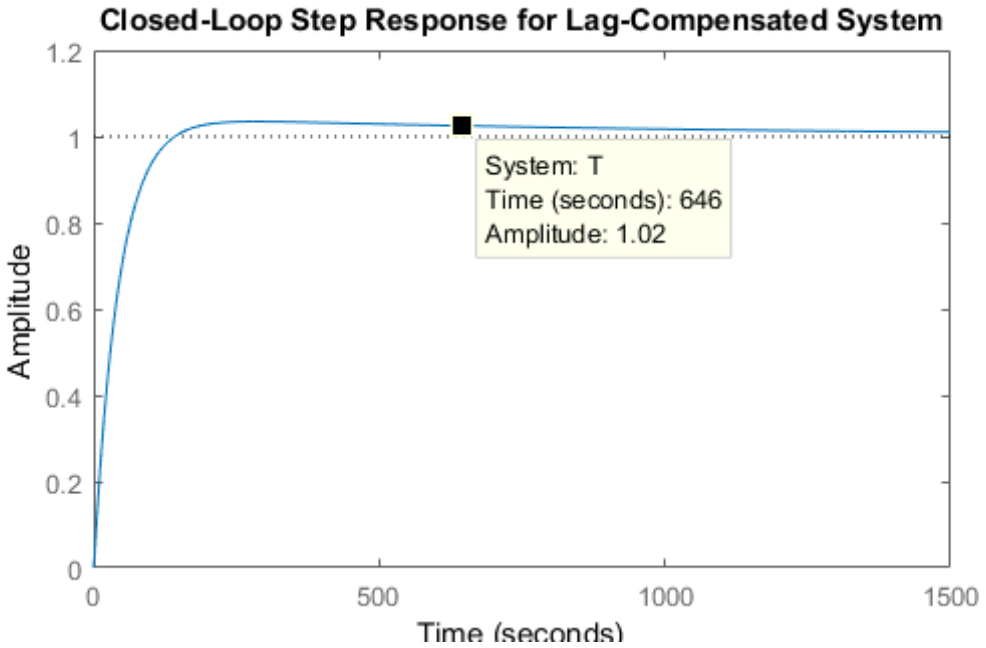

Figure 11: Lag compensation dramatically increases settling time.

2. From this, calculate the required gain K. In MATLAB, this was performed by multiplying the original transfer function by s, then setting `K=dcgain(Kv/sG)` for this Type 1 system.

3. The required phase margin P, phase angle ϕ, and bandwidth ω_{BW} were computed from the T_s and % OS specifications, using 2nd order formulae [1]. However, add an initial 10 degrees to P to account for the fact that the addition of a lead compensator itself affects the system's phase margin frequency. This value can be adjusted if necessary afterwards.

4. The current phase margin p was obtained from the Bode plots of the system `KG`. The required phase contribution ϕ_c is P - p. From this, calculate a value for β, given:
$$\beta = \frac{1 - \sin(\phi_c \pi / 180)}{1 + \sin(\phi_c \pi / 180)} \tag{22}$$

5. Find the new phase margin frequency ω_{max} by locating the frequency where the magnitude of `KG` is equal to the negative of the magnitude at the peak of the compensator's phase curve.

6. Now, the new break frequencies can be located as $T = 1/(\omega_{max}\sqrt{\beta})$. Equiva-

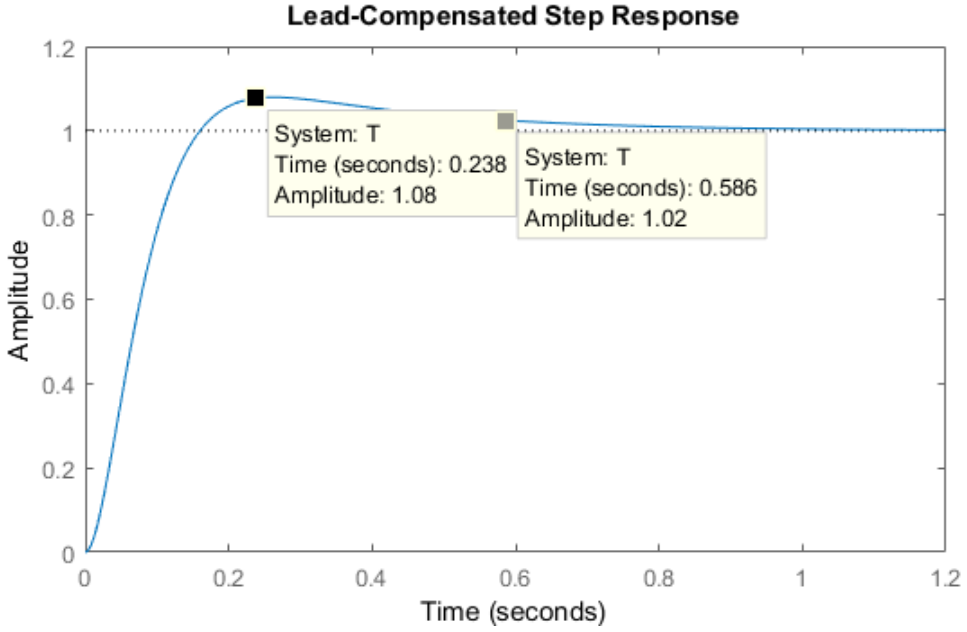

Figure 12: 8% OS, $T_s = 0.59$s: Where the correction factor to desired phase margin was estimated as 10 degrees, the system undermet its specifications.

lently, the lead compensator can be given as:

$$G_c(s) = K_c \frac{s + \omega_L}{s + \omega_H} \tag{23}$$

Then, the break frequencies are: $\omega_L = \omega_{max}\sqrt{\beta}$, $\omega_H = \omega_L/\beta$, and the gain of the lead compensator is $K_c = 1/\beta$.

The first trial yielded a response that undermet the system requirements. Its overshoot was 8% and the settling time was 0.59s (Fig. 12). At first, various adjustments to K_v, T_s and % OS were made. One could either decrease % OS and T_s, but not as effectively as increasing K_v and decreasing % OS (Appendix A). Then, it was realised that the correction factor for the desired phase margin may not be correct. Adjusting this to 20 degrees (as opposed to 10) immediately yielded the desired system response (Fig. 13). It was observed that the effect was to put the compensator's pole almost double the distance further away. The final controller is:

$$G_c(s) = 32.821 \frac{s + 3.165}{s + 103.866} \tag{24}$$

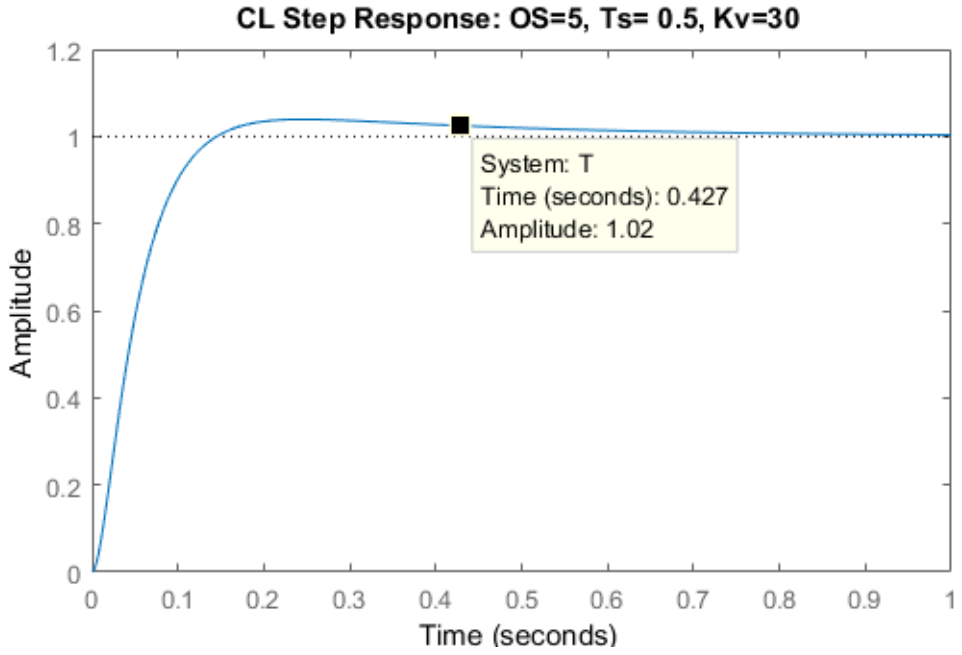

Figure 13: 4% OS, $T_s = 0.43$s: Where the correction factor to desired phase margin is 20 degrees, the system met its specifications.

(c) Method Suitability

A lead controller has been designed that gives 4% OS and a settling time of 0.43 seconds. Therefore, the specifications have been met. The frequency response method has proved highly suitable for this problem, because the problem is second order so that second order equations and assumptions could be used. Further investigation could optimise control effort for these specifications by varying K_v, the correction factor, and the specified % OS and T_s.

2.2 Including the Dynamic Effects of Solar Panels

(a) $\theta_s(s)/T(s)$

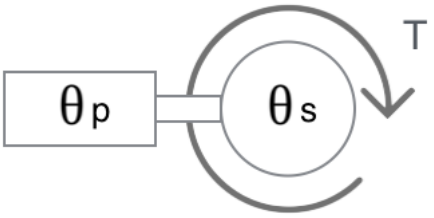

Figure 14: The satellite-solar panel symmetric model showing applied torque T.

From the symmetric model shown (Fig. 14), the system equations are:

$$J_s\ddot{\theta}_s = T - k\theta_s - d\dot{\theta}_s + k\theta_p + d\dot{\theta}_p \tag{25}$$

$$J_p\ddot{\theta}_p = -k\theta_p - d\dot{\theta}_p + k\theta_s + d\dot{\theta}_s \tag{26}$$

These have been derived similarly to the quarter-car model of Assignment 1, by considering the forces on the satellite, then the solar panel. Expressing these in the Laplace domain and equating them results in the transfer function:

$$\frac{\theta(s)}{T(s)} = \frac{\frac{1}{J_s}s^2 + \frac{d}{J_sJ_p}s + \frac{k}{J_pJ_s}}{s^4 + \frac{J_p+J_s}{J_sJ_p}ds^3 + \frac{J_p+J_s}{J_sJ_p}ks^2} \tag{27}$$

(b) State Space Controller

Because of the single-input multiple-output system, a state space model was trialled. The following specifications were taken:

- $\omega_n = 0.2$ rad/s
- $J_s = 0.4352$ kg m^2
- $J_p = 9.083$ kg m^2
- $k = \omega_n^2 J_p$ N/m
- $d = 1 \times 10^-3$ Ns/m

First, a system without integral control was investigated. Then, a system with integral control was designed.

Without Integral Control

The state matrices are:

$$\dot{\mathbf{x}} = \mathbf{A}\mathbf{x} + \mathbf{B}u,\ \mathbf{x} = \begin{bmatrix} \theta_s \\ \dot{\theta}_s \\ \theta_p \\ \dot{\theta}_p \end{bmatrix} \tag{28}$$

$$y = \mathbf{C}\mathbf{x} \tag{29}$$

$$\mathbf{A} = \begin{bmatrix} 0 & 1 & 0 & 0 \\ -k/J_s & -d/J_s & k/J_s & d/J_s \\ 0 & 0 & 0 & 1 \\ k/J_p & d/J_p & -k/J_p & -d/J_p \end{bmatrix} \tag{30}$$

$$\mathbf{B} = \begin{bmatrix} 0 \\ 1 \\ 0 \\ 0 \end{bmatrix} \tag{31}$$

$$\mathbf{C} = \begin{bmatrix} 1 & 0 & 0 & 0 \end{bmatrix} \tag{32}$$

Completing the controllability and observability matrix informs that the model is both controllable and observable. The system is fourth order and without a controller, is highly oscillatory with a pole on the origin. To design for 5% OS and $T_s = 0.5$s, 2nd order formulae were used which located the desired dominant poles at $-6.2832 \pm 6.5891i$. Two additional poles were added at the locations of the zeros: $-0.0001 \pm 0.2000i$.

To find the values of the K matrix, compare the characteristic equation of the system with that of the desired pole placements. This was performed conveniently using the `place()` function in MATLAB. The closed-loop system was then evaluated as:

$$\dot{\mathbf{x}} = (\mathbf{A} - \mathbf{B}\mathbf{K})\mathbf{x} + \mathbf{B}r \tag{33}$$

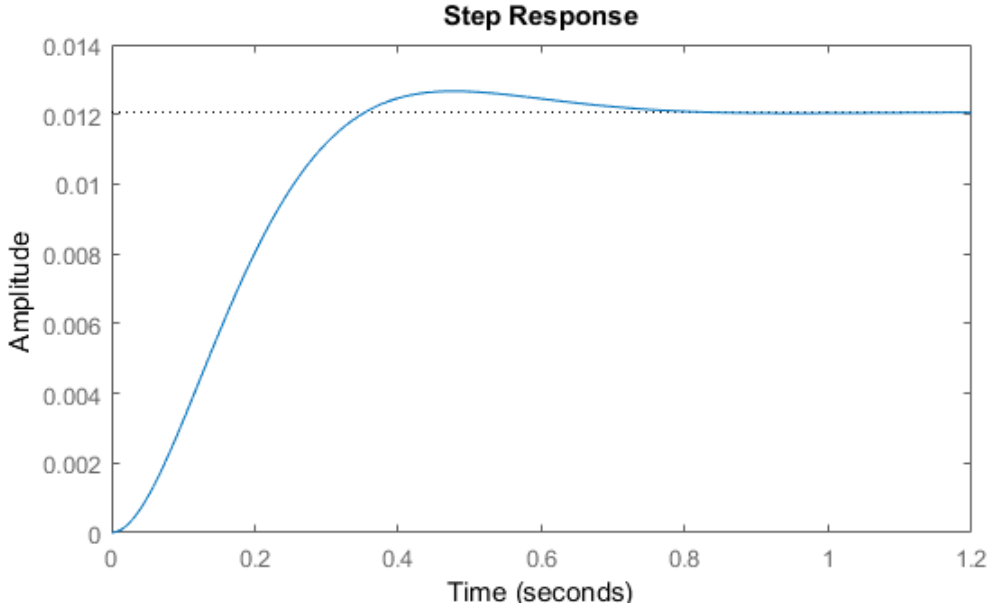

Figure 15: Step response for state space controller without integral control has a steady-state error of 0.0001.

$$y = \mathbf{C}\mathbf{x} \tag{34}$$

The step response shown in Fig. (b). It is pleasing that the controller has acted to stabilise the system. The system has an overshoot of exactly 5% but a slightly longer settling time than the specified 0.5s. Also, there is a steady-state error of 0.0001. Accuracy is typically very important to satellites; a minute error in θ_s could amount to kilometres of difference in the object it is tracking. Therefore, the problem is repeated to include integral control.

With Integral Control

To add integral control, an additional state variable must be added so that the error is its derivative (Fig. 16): $\dot{x}_N = -\mathbf{C}\mathbf{x} + r$. Now, the phase-variable representation is:

$$\begin{bmatrix} \dot{\mathbf{x}} \\ \dot{x}_N \end{bmatrix} = \begin{bmatrix} (\mathbf{A} - \mathbf{B}\mathbf{K}) & \mathbf{B}K_e \\ -\mathbf{C} & 0 \end{bmatrix} \begin{bmatrix} \mathbf{x} \\ x_N \end{bmatrix} + \begin{bmatrix} \mathbf{0} \\ 1 \end{bmatrix} r \tag{35}$$

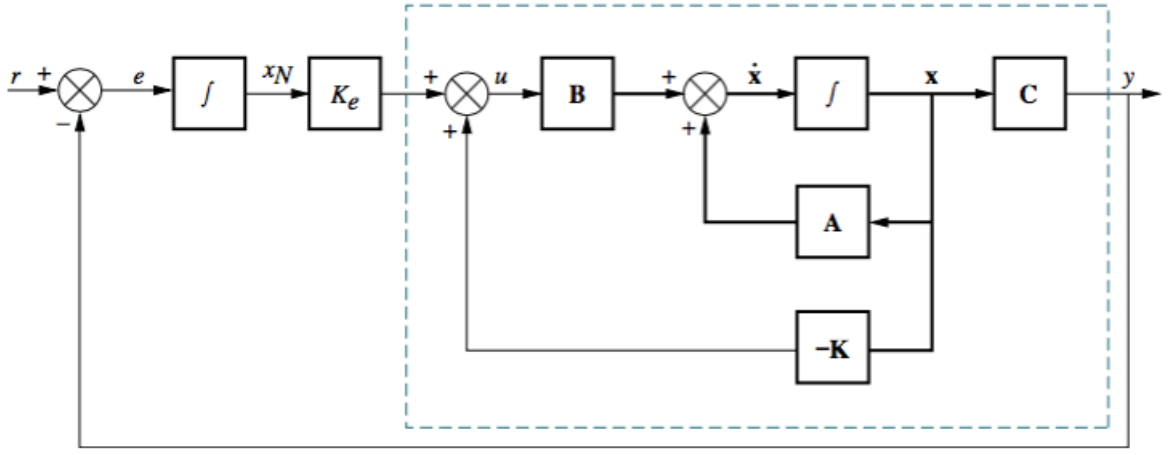

Figure 16: Block diagram of system with integral control [1].

$$y = \begin{bmatrix} \mathbf{C} & 0 \end{bmatrix} \begin{bmatrix} \mathbf{x} \\ x_N \end{bmatrix} \tag{36}$$

Equivalently, define new matrices:

$$\dot{\mathbf{x}}_\mathbf{a} = (\mathbf{A}_a - \mathbf{B}_a\mathbf{K}_a)\mathbf{x}_a + \mathbf{B}_r r \text{ where } \mathbf{x} = \begin{bmatrix} \theta_s \\ \dot{\theta}_s \\ \theta_p \\ \dot{\theta}_p \\ x_N \end{bmatrix} \tag{37}$$

$$y = \mathbf{C}_a\mathbf{x}_a \tag{38}$$

where $\mathbf{A}_a$, $\mathbf{B}_a$, $\mathbf{B}_a$, and $\mathbf{C}_a$ are augmented counterparts of the original and the vector multiplying the reference input is $\mathbf{B}_r$:

$$\mathbf{A}_a = \begin{bmatrix} 0 & 1 & 0 & 0 & 0 \\ -k/J_s & -d/J_s & k/J_s & d/J_s & 0 \\ 0 & 0 & 0 & 1 & 0 \\ k/J_p & d/J_p & -k/J_p & -d/J_p & 0 \\ 1 & 0 & 0 & 0 & 0 \end{bmatrix} \tag{39}$$

$$\mathbf{B}_a = \begin{bmatrix} 0 \\ 1 \\ 0 \\ 0 \\ 0 \end{bmatrix} \tag{40}$$

$$\mathbf{C}_a = \begin{bmatrix} 1 & 0 & 0 & 0 & 0 \end{bmatrix} \tag{41}$$

$$\mathbf{B}_r = \begin{bmatrix} 0 \\ 0 \\ 0 \\ 0 \\ -1 \end{bmatrix} \tag{42}$$

A fifth pole was placed to match the new system order, at a relatively far location from the rest, $-10 \pm 0i$. The new gain matrix $\mathbf{K}_a$ was again formed using `place()` and the closed-loop step response plotted, this time adjusting the desired settling time to $T_s = 0.3$ s to ensure it meets the specification. Figure 17 shows that the system now clearly meets the overshoot and settling time requirements with zero steady-state error.

Nonetheless, the excellent performance of the controller comes with the cost of high control effort. Figure 18, at one point, shows a torque of almost 50 Nm necessitated. For satellite attitude control, torques that can be achieved using reaction wheels are within the order of 0.02-2 Nm [2]. Therefore, the stated requirements for overshoot and settling time are not reasonable - the necessary control input is magnitudes higher than that feasible in practice.

Adjusting the Control Effort

The state space model with integral control was re-created to yield reasonable torques between 0.02-2 Nm. As evident through Figs. 19 and 20, the more the torque is restricted, the larger the settling time (for the same percentage overshoot).

It was also found that reducing the desired % OS resulted in a lesser maximum torque. In general, the torque was observed to initially spike up to a maximum then adjust to a continual cycle of lesser amplitude. For the same specified settling time of 2.6s, decreasing the % OS to 0.1 (almost critical damping) reduced the maximum torque without a significant effect on the actual settling time (Fig. 21).

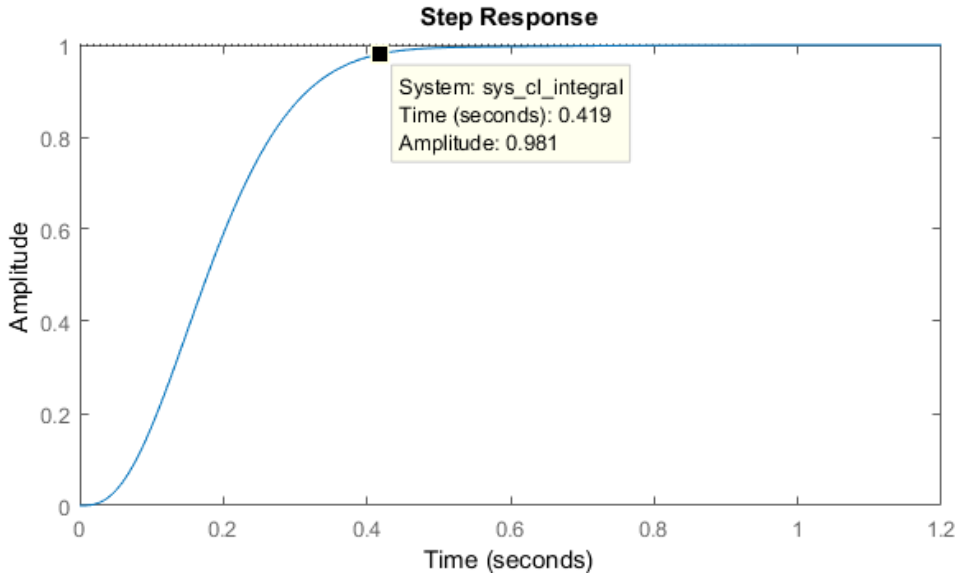

Figure 17: The step response with integral control meets the overshoot and settling time requirements with zero steady-state error.

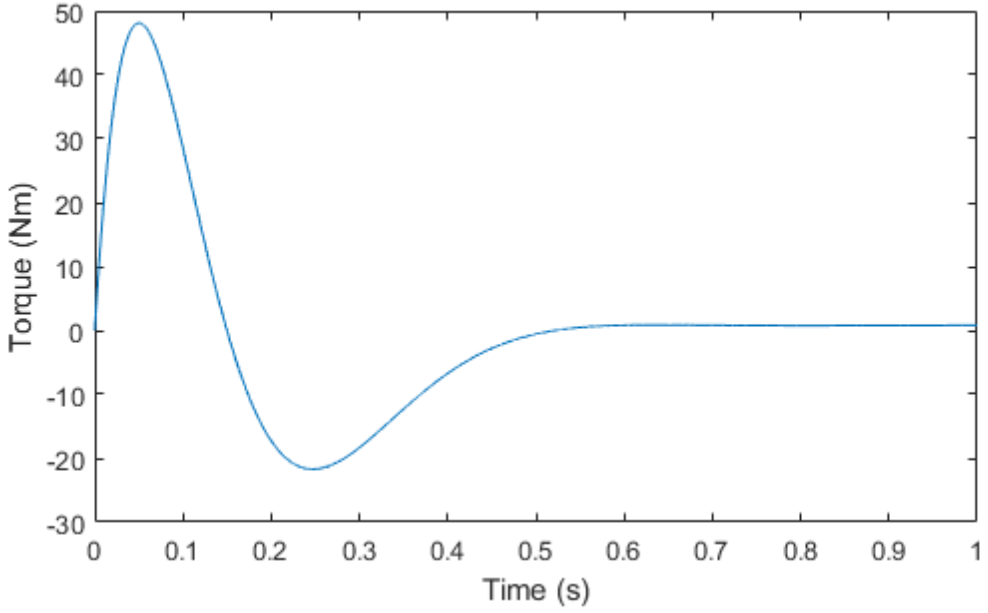

Figure 18: The control effort is extremely high. The torque is at maximum almost 50 Nm.

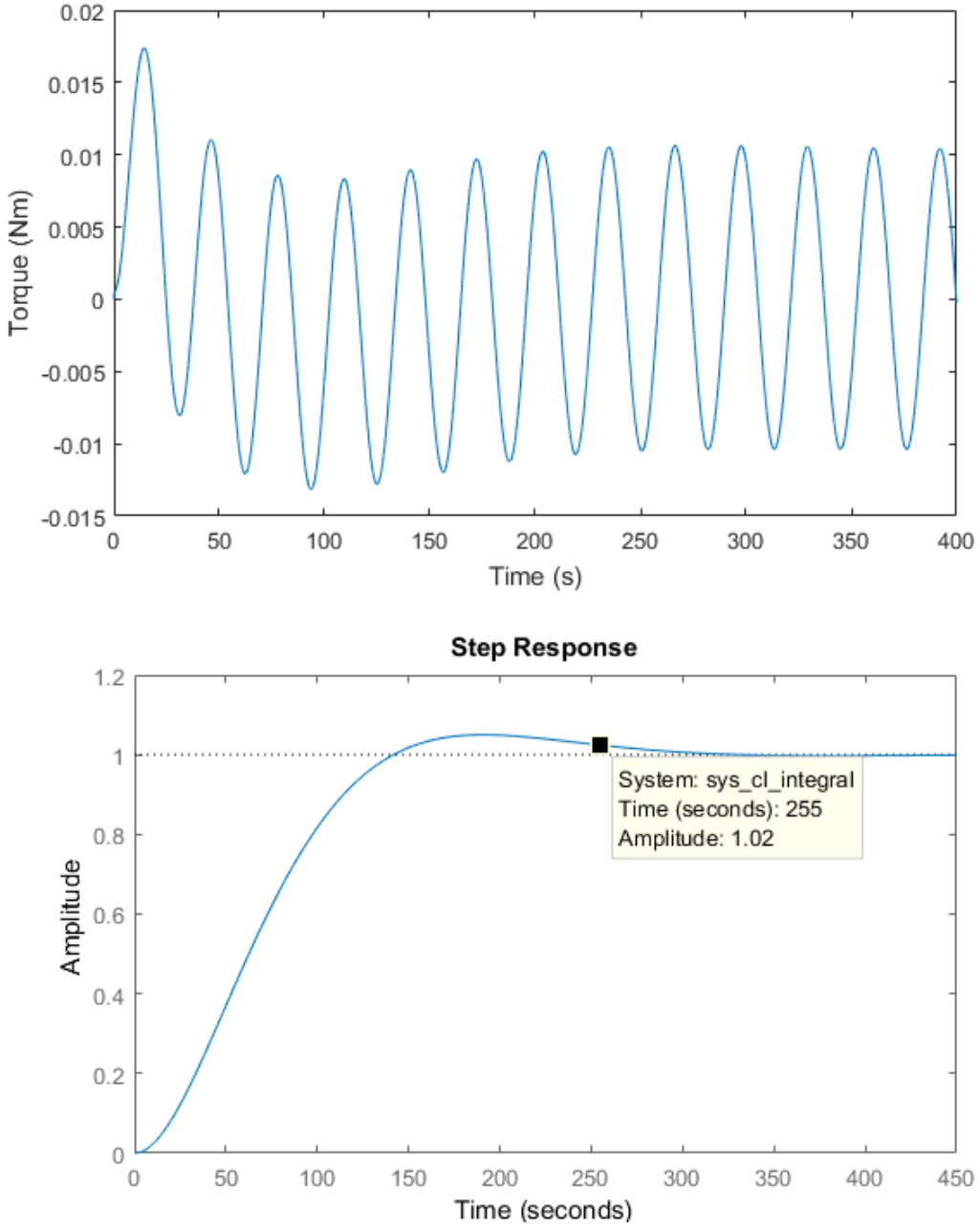

Figure 19: System with torque output less than ±0.02 Nm, has 5% OS and T_s = 255s.

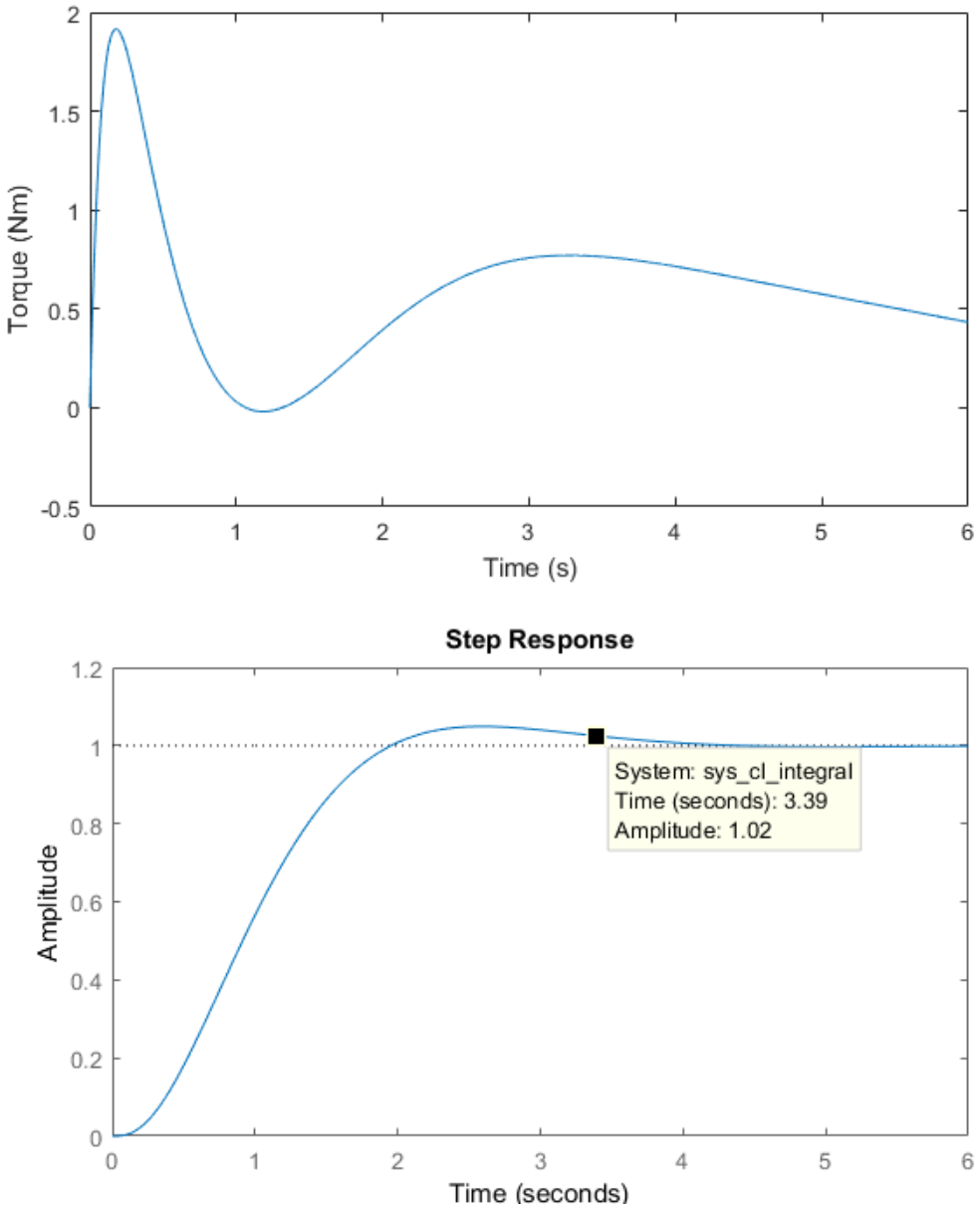

Figure 20: System with torque output less than ±2 Nm, has 5% OS and $T_s = 3.39$s.

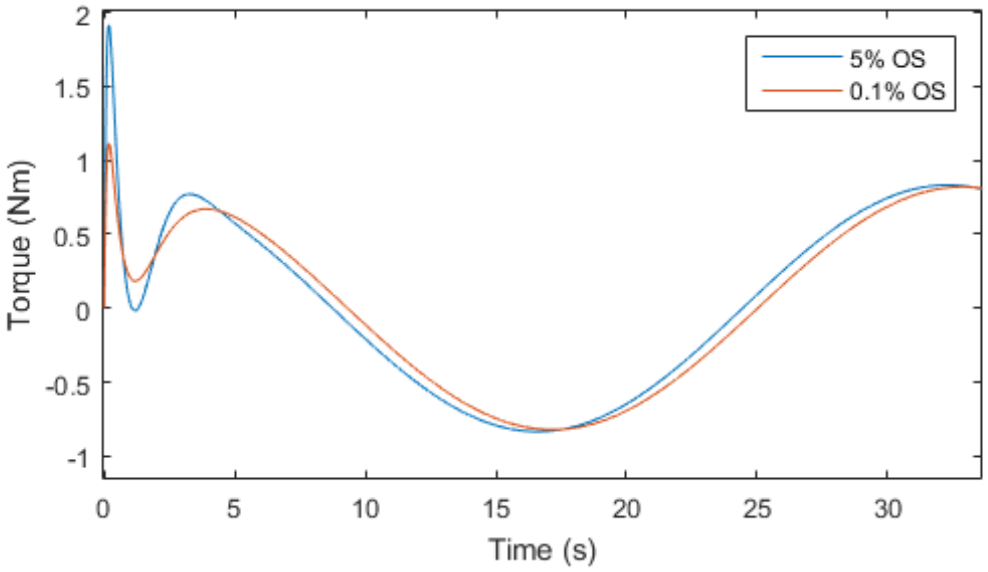

Figure 21: For the same specified T_s, reducing the % OS specification reduces the maximum applied torque (control input) required.

The closed-loop step response of the 0.1% (negligible) OS, $T_s = 2.6$s system is also shown (Fig. 22). Its actual settling time is 3.74s. This is therefore the proposed system once control effort has been considered, which minimises the applied torque by extending the settling time, and allows a minimum-specification reaction wheel by decreasing the overshoot. Its gain matrix K_a is:

$$\mathbf{K}_a = \begin{bmatrix} 25.09 & 12.41 & 0.87 & 0.06 & 17.62 \end{bmatrix} \tag{43}$$

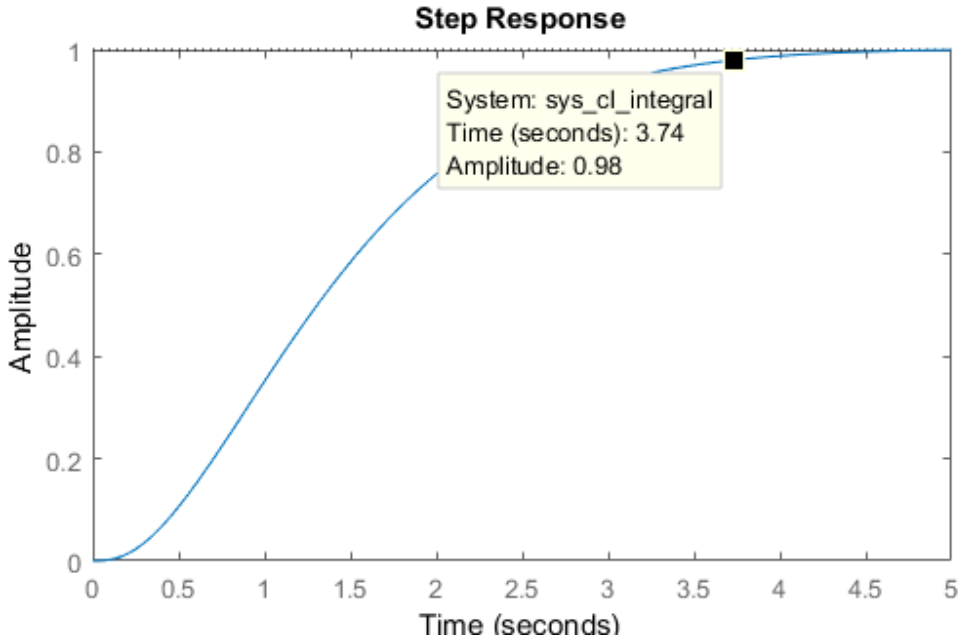

Figure 22: Proposed system: 0.1 % OS, $T_s = 2.6$s closed-loop step response with actual settling time of 3.74s.

(c) Noise & Disturbance

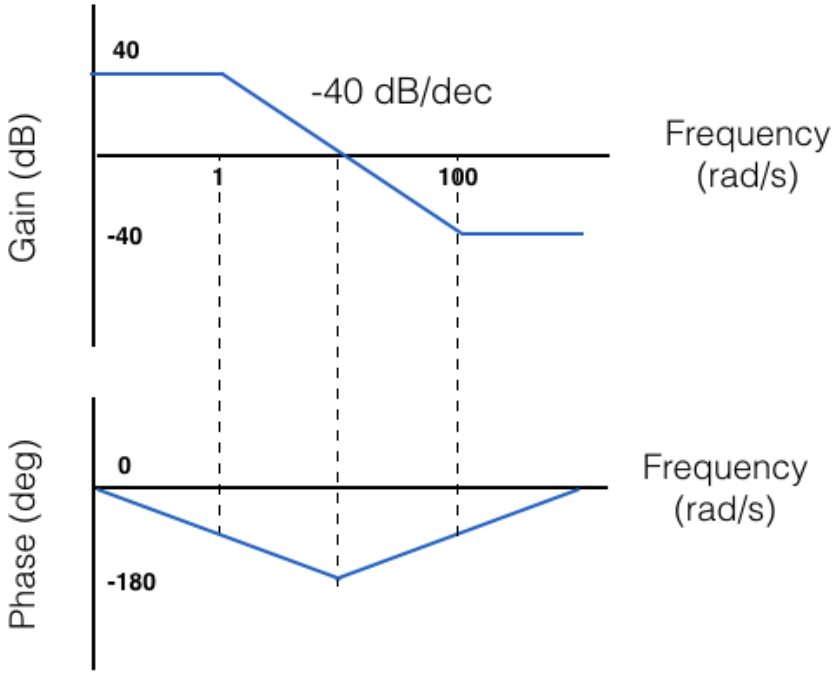

Figure 23: The proposed system must have a phase drop to -180 degrees.

Plotting the proposed system shows that the suggestion is not feasible (Fig. 23). If the gain is to change from 40 dB to -40 dB within the span of two decades, the rate of change is -40 dB/decade. However, due to Bode's Gain-Phase relation, the phase must decrease to -180 degrees for -40 dB/decade of gain reduction [3]. This in fact will make the system highly oscillatory and unstable.

Therefore, while it is ideal to have low gain at high frequencies, there can not be such a sharp gradient such that the phase lag is 180 degrees. The gradient must therefore be shallower than 40 dB/decade.

2.3 Docking to Refuel the Satellite

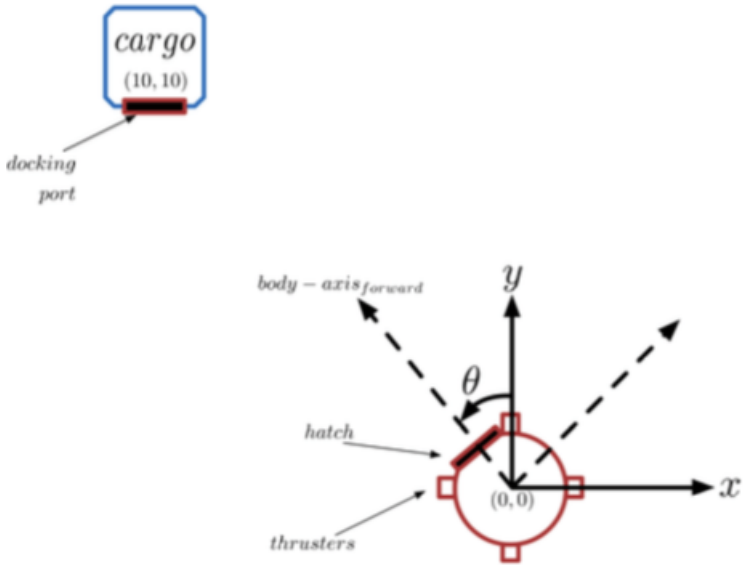

Figure 24: Diagram for satellite docking, take θ in the opposite direction shown.

The problem schematic is given is Fig. 24, however, take θ in the opposite direction than as shown. The schedule is:

1. To first move the satellite linearly using the thrusters F_x and F_y, accelerating then decelerating the unit to ensure $v = 0$ at the docking port and the position $x = 10$ in both x & y coordinates.
2. Once the satellite unit is stationary, rotate it in θ to achieve 45 degrees to face the docking port.

The results are shown through Figs. 25 to 29. The modelling procedure utilised the following:

- Zero gravity assumption (low earth orbit), zero resistance to thrusters overall
- Force is translational and can be summed for each thruster about the same axis, so that F_x is the sum of thrust force acting in x and F_y is the sum of thrust force acting in y.
- Analogously, the linear traverse can be simplified to $F_x = F_y$ to accelerate and decelerate to (10,10).

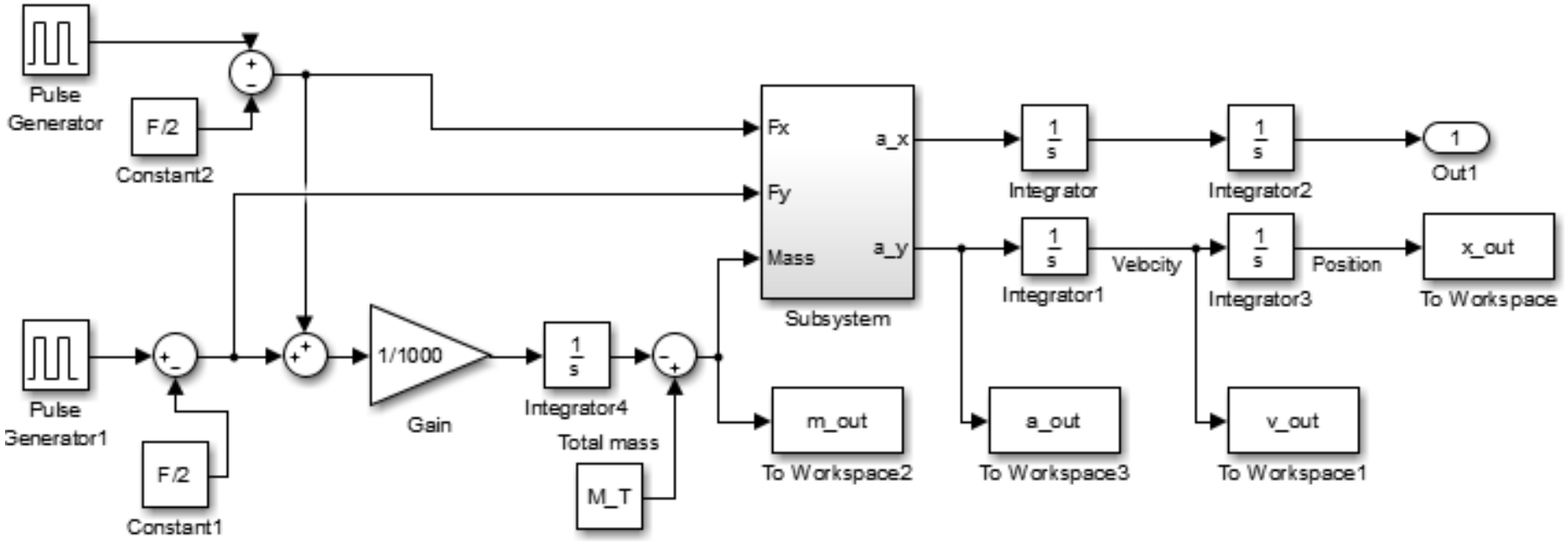

Figure 25: The linear simulation.

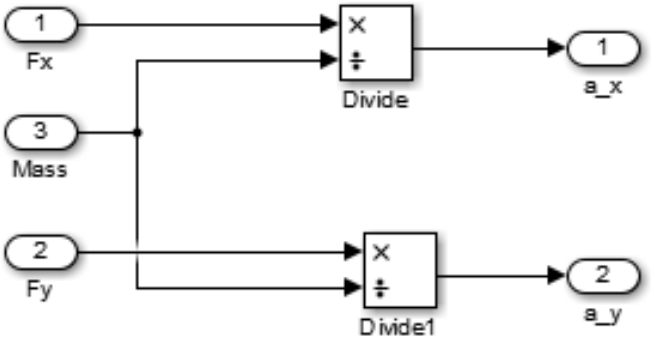

Figure 26: The subsystem of the linear simulation.

The reduction in mass with fuel consumption was also considered. The linear system can be expressed as:

$$F_x = F_L + F_R = m\ddot{x} \tag{44}$$

$$F_y = F_T + F_B = m\ddot{y} \tag{45}$$

$$m = -\int \alpha(F_x + F_y) + M_T \tag{46}$$

where L and R refer to thrusters acting in x and T and B refer to thrusters acting in y; m is the total mass of the unit; α is a constant which relates the fuel consumption with the thrust forces; M_T is the total initial mass of the unit, the sum of masses of the reaction wheel, satellite, solar panels, and initial fuel load.

For the linear simulation, the force input was modelled via manipulating a pulse generator unit to essentially provide a square wave of amplitude 24 and a period of 20 s. By moving this square wave down 12, a reference input was created of an initial 12 N, then at 10s, a step decrease to -12 N to provide the acceleration and deceleration reference points. This and the corresponding velocity and position outputs are shown together in Fig. 27. This 12 N force on each F_x and F_y was found to achieve the traverse of 10 m in each x and y in a period of 20 s.

Because the unit is now stationary at (10,10), we can rotate the satellite 45 degrees to achieve the objective using the same control system as that designed in **2.2**. In **2.2**, it was found that the satellite would rotate 1 degree (step response shown) in

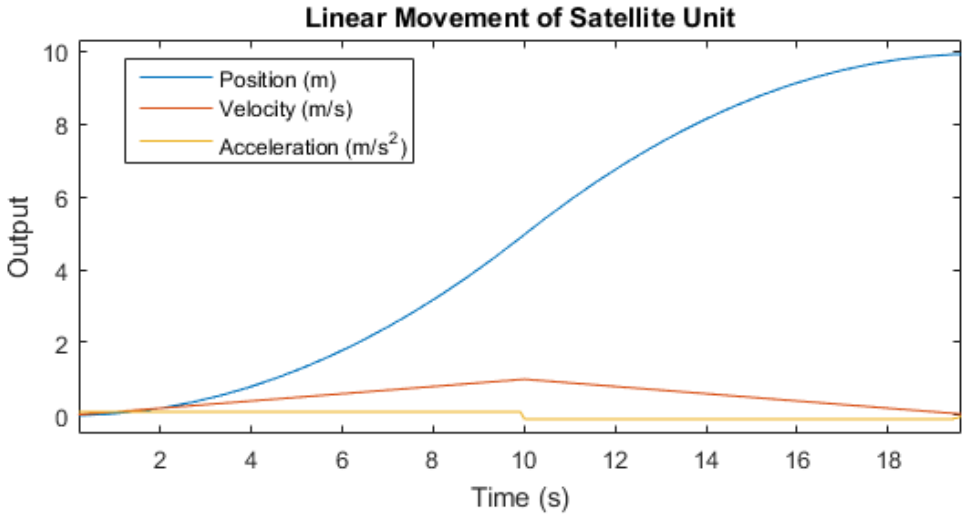

Figure 27: Results of the linear simulation.

3.74 s. Therefore, to rotate 45 degrees, allow 4×45 s, rounding the settling time up to 4 to ensure that the steady-state error has settled to 0. The input is therefore a ramp, where the reference value increases by 1 degree after every 4 s. This is shown as well as the received θ_s response and the necessary input torque in Figs. 28 and 29.

The bumps that are visible in the position output are the shapes the system settling after each reference value has been changed; the time step was set sufficiently small to ensure no graphical discretisation errors.

Overall, via the system used to model the docking of the satellite, it can be said that the objective has been achieved. By allowing the linear motion to occur first, followed by rotation, permits a simplification to an otherwise complex problem where multiple forces are involved in a rotational system. The way the question was modelled, the reference thrust was equal to the output applied thrust, without variations caused by typical system dynamics. Therefore, a controller was not needed for this linear system. With more knowledge about the appropriate dynamics of thrusters, the problem could be remodelled, which may then necessitate a control system.

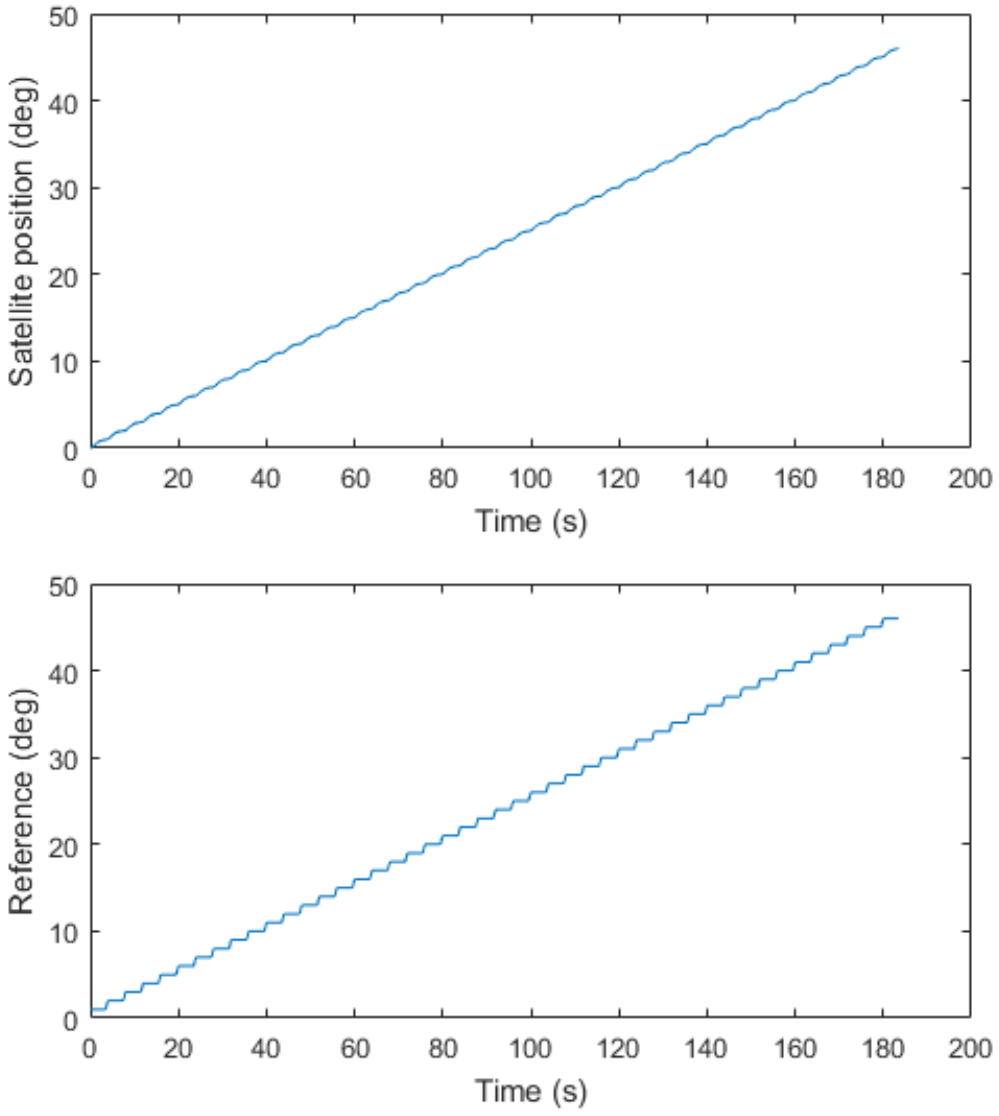

Figure 28: Satellite unit position over time, achieving 45 degrees and the reference angles generated.

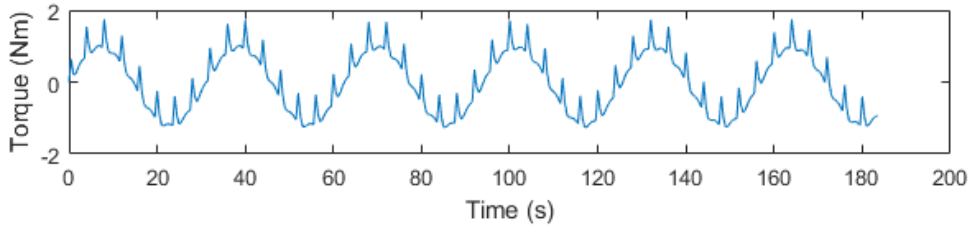

Figure 29: The applied torque input over time.

3 Lab Report

3.1 Lab 2

(a) P Control

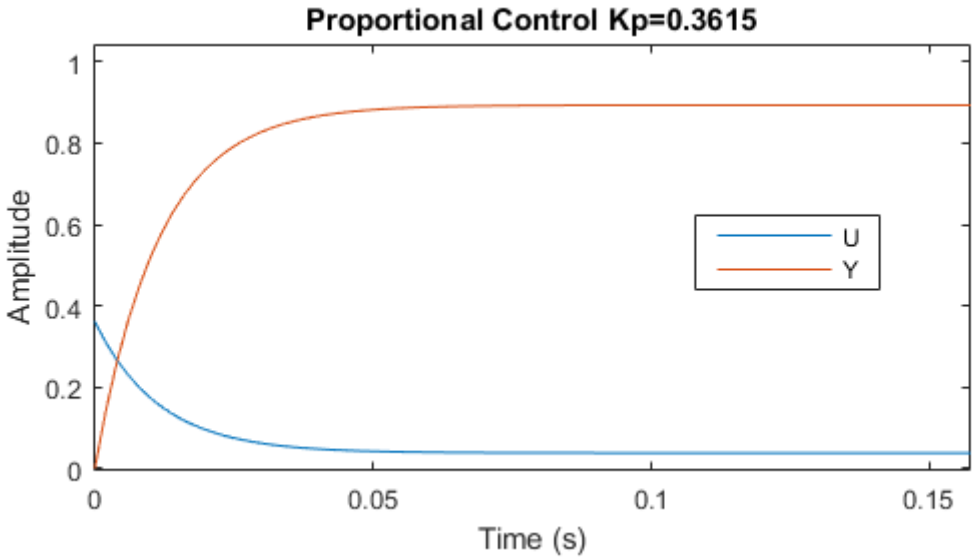

Figure 30: Output Y & input U with $K_p = 0.36$.

A proportional controller $u = eK_p$ amplifies the error signal, which essentially speeds up the system and improves steady-state error. Increasing the gain K_p from 0.1 to 1 reduced the steady-state error and improved the transient response. However, when the gain was increased to 5, it caused the system to become highly oscillatory, but eventually settled with even lower steady-state error. The gain calculated in the pre-work was $K_p = 1/(\tau K_{ss})$, for 16% OS. For $\tau = 0.12$s and K_{ss}=23.05, this equates to $K_p = 0.36$. The response with its input is shown in Fig. 30. When physically interacting with the system, some resistance was observed. Theoretically, this would be a constant resistance due to having constant gain as a controller.

(b) D Control

A derivative controller expresses itself as $u = K_d(de/dt)$. It acts on the derivative of the error signal, therefore acts upon a prediction of the system. This can therefore speed up the response of the system, but can also cause instability when the signal

is noisy, the derivative gain is too high, or the rate of derivative control demanded is too high for the control loop rate, which are analogous ideas. This is as seen in the derivative-controlled step response for this system, which is shown with the remaining step responses for this lab in Appendix B.

The figure shows that the derivative controlled response is initially oscillatory, but then settles quickly to a steady-state value. It is hypothesised that in the initial response, the error was changing significantly, so the derivative control system acted strongly within a limited loop rate, driving it to under- and over-shoot. Another explanation is that trying to speed up the response drives the closed loop poles further away from the real axis, generating the initial oscillation.

Again, some resistance was sensed when interacting the unit. In theory, derivative control offers more resistance to a higher derivative of the error. In this case, resistance is proportional to the applied disturbance torque.

(c) PD Controller

PD control can be expressed as $u = eK_p + K_d(de/dt)$. The steady-state value was above 1. There was a large overshoot, but a very fast settling time. The controller combines the mechanisms of P and D control in series, so can be thought to have the benefits/disadvantages of both. This system will provide resistance proportional to the disturbance size as well as to its velocity.

(d) PID Controller

The PID-controlled system exhibited an initial spike, followed by a rise to the steady-state value with zero error. The spike is due to the fact that dynamics were acting on two different time scales. The first spike is attributed to the PD controller, and the slower convergence is a result of the integral action. With an integrator, the resistance to disturbance also theoretically increases over time, as integrators by definition act upon the accumulation of error until the error is zero.

3.2 Lab 3

(a) Aim

A controller must be designed for a crane which needs to pick up a very light objects at the bottom of its pendulum, then place it in its target location. To successfully reach the target, the tip of the pendulum must be stationary and θ must be at the reference angle (Fig. 41). References are given by the REFGEN block. A sequence of four pick-up/drop-off locations are given. The task is to control the crane so that it does this in the least time possible. System equations and given parameters are available in Appendix C.

(b) Method

Because state space methods were not well known at the time of the laboratory, a root locus method was first trialled. It was soon apparent that the method was not suitable. For instance, the following transfer function was obtained for $\theta(s)/U(s)$:

$$\frac{\theta(s)}{U(s)} = \frac{Ds^2 + (BH - DF)s + CH - DG}{s^4 - (A + F)s^3 - (G + BE - AF)s^2 + (AG - CE)s} \tag{47}$$

where, negative signs included, $A - D$ are coefficients of the RHS of Eq. 49 and $E - H$ are those of Eq. 50.

This produced the root locus of Fig. 31. However, having followed the generic procedure to place compensator poles and zeros, it was found that the root locus afterwards did not go through the desired locations (Appendix C). The difficulty in using the root locus method for this problem is attributed to the complex zeros near the dominant poles. It is thought that the use of a notch filter might improve the success of the root locus method. The full attempt is available in `Lab3_RL.m`.

As a result, in the laboratory, a trial and error method was taken where θ was tuned for first, then α. A PID system was elected for both. An approximate aim was to run the REFGEN program in less than 10 seconds.

(c) Results

The control system shown in Fig. 33 successfully completed the REFGEN program in 7.2 seconds. Gain values of the achieved system were for θ: $k_p = 4$, $k_i = 8$, and

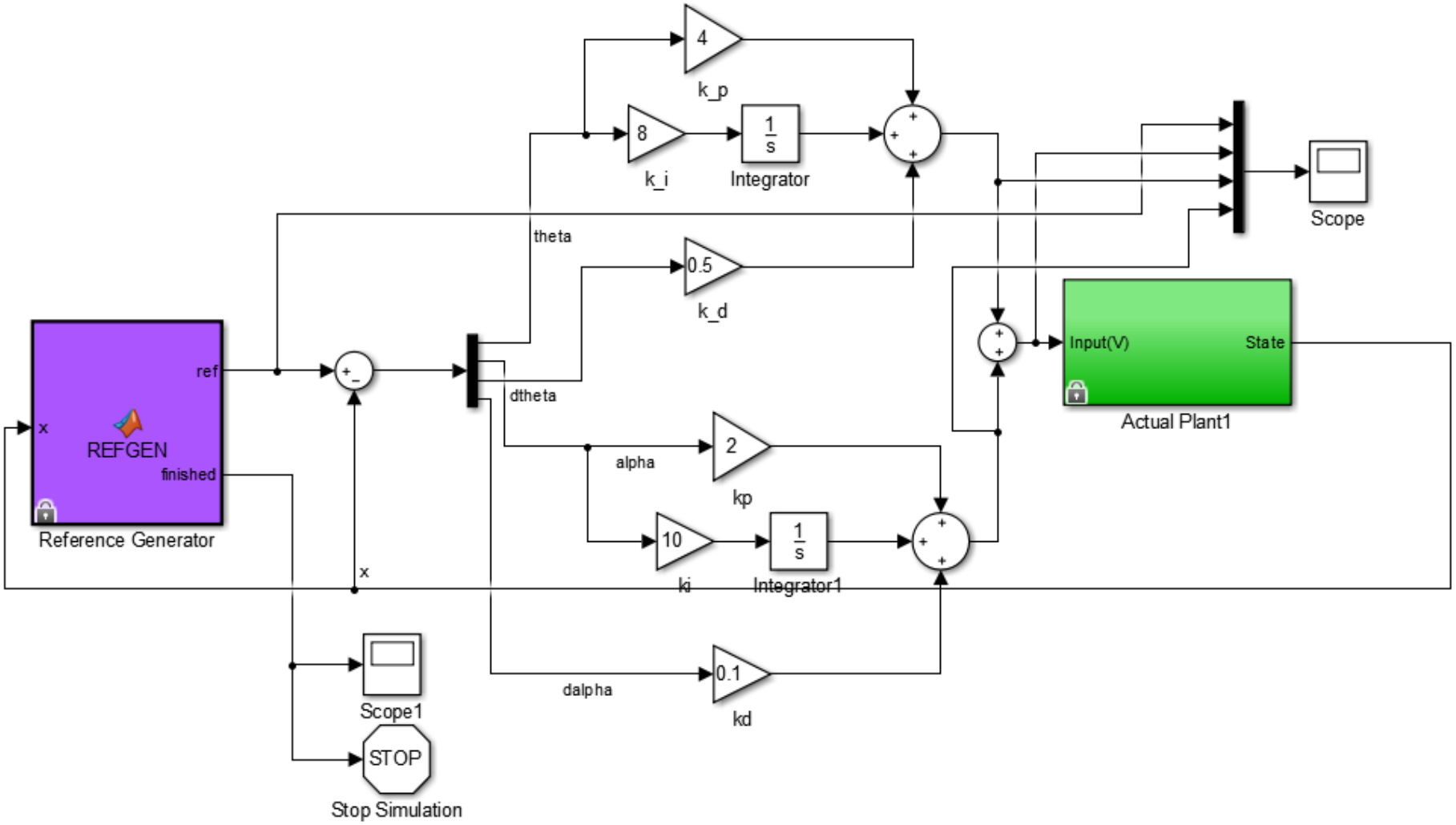

Figure 33: Simulink model for Lab 3, showing selected gains.

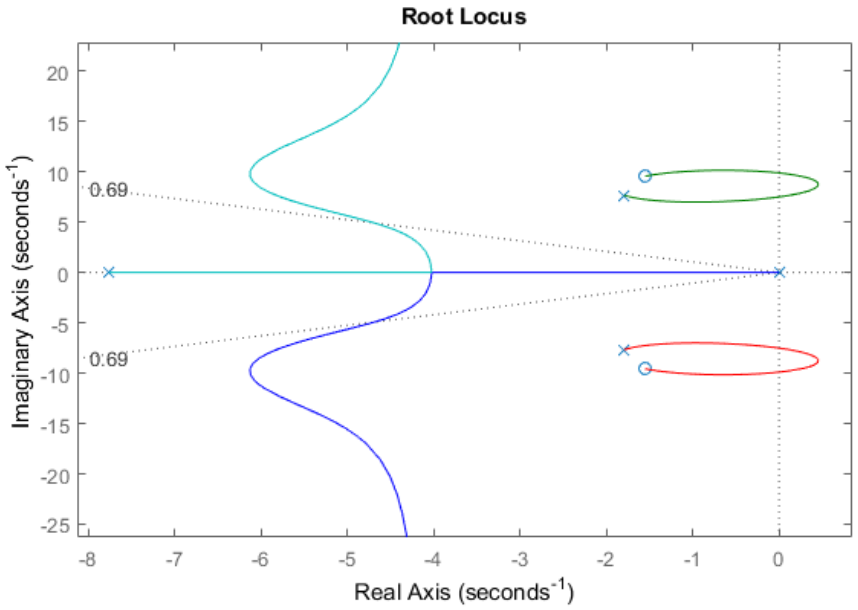

Figure 31: Open-loop root locus for the crane system, with 5% OS line shown.

$k_d = 0.5$. For α, these were: $k_p = 2$, $k_i = 10$, and $k_d = 0.1$. Appendix C includes a plot of the generated θ, α, $\dot{\theta}$, $\dot{\alpha}$, and the control input u.

(d) State Space

After the laboratory, a state space model was investigated. In phase-variable form:

$$\begin{bmatrix} \dot{\theta} \\ \dot{\alpha} \\ \ddot{\theta} \\ \ddot{\alpha} \end{bmatrix} = \begin{bmatrix} 0 & 0 & 1 & 0 \\ 0 & 0 & 0 & 1 \\ 0 & C & A & B \\ 0 & G & E & F \end{bmatrix} \begin{bmatrix} \theta \\ \alpha \\ \dot{\theta} \\ \dot{\alpha} \end{bmatrix} + \begin{bmatrix} 0 \\ 0 \\ D \\ H \end{bmatrix} u \tag{48}$$

A controller was formed using the same method as in **2.3**, without integral control. The procedure is available for inspection in `State_Space.m`. Two poles were placed at desired dominant pole location, the other two were placed to cancel the zeroes of $\theta(s)/U(s)$. The Simulink model was modified so that reference values were fed into gain matrix $\mathbf{K}$ as shown in Fig. 45 of Appendix C.

Program completion times are shown for various input specifications in Fig. 32. While one would expect faster program completion by decreasing settling time, it

OS (%)	T_s (s)	Program completion (s)
5	1	24
5	0.25	Inf.
2	1	23.3
2	0.5	18
2	0.25	29
1	0.7	19.54
1	0.5	17.5
1	0.25	25.2

Figure 32: Program completion times for various input specifications.

was found that this caused the θ arm to move quickly, generating high oscillatory motions for the α arm. Because reference values were not loaded until $\dot{\alpha} = 0$, a longer amount of time was spent waiting for the α arm to settle. The fastest program run tested occurred when the overshoot about θ was minimal (1%) and the specified settling time was not too high nor too low. By state-space, a program completion time of 17.5 s was achieved using the at-home simulator block.

Therefore, while state space provided a somewhat more methodical approach to controller design, in this case the trial and error approach in fact yielded a better (faster) result via the use of a PID controller for each θ and α, where control over α is not, in reality, direct. In state space, it is envisaged that placing the additional poles at the zeroes of $\alpha(s)/U(s)$ would better affect α, however, at the cost of diminished control of θ. In this way, the state space model is still limited to its 2nd order assumptions. Nevertheless, to affect α similarly to the PID system, a nested state space controller could be investigated.

References

[1] N. Nise, *Control Systems Engineering*. Wiley, 2011.

[2] M. Sidi, *Spacecraft Dynamics and Control: A Practical Engineering Approach*. Cambridge Aerospace Series, Cambridge University Press, 1997.

[3] B. Lurie and P. Enright, *Classical Feedback Control: With MATLAB*. Automation and Control Engineering, Taylor & Francis, 2000.

4 Appendices

Visit `https://github.com/sojung21/amme3500` to access all Simulink models and MATLAB code.

A Q2.1(b) Additional Plots

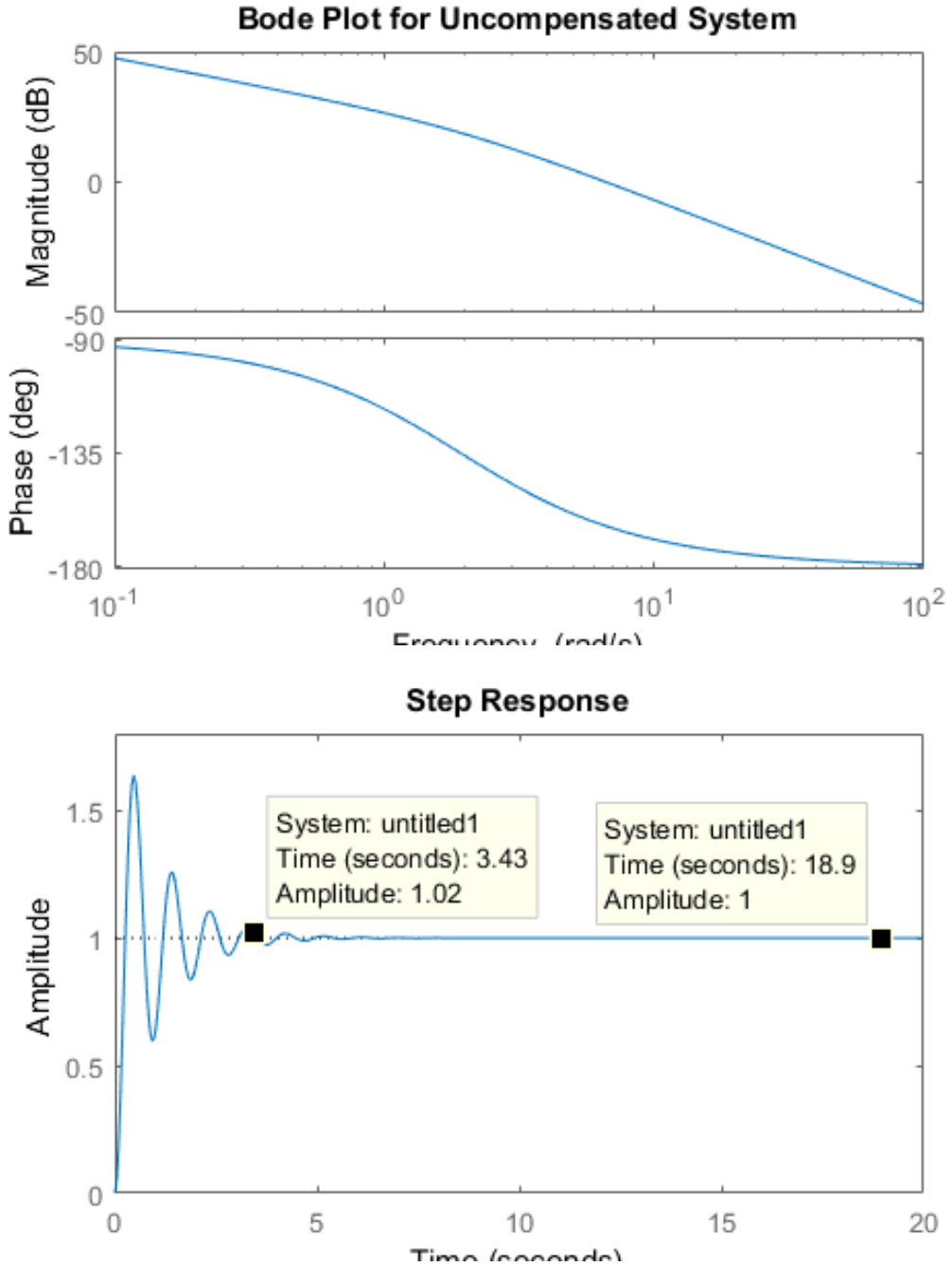

Figure 34: The uncompensated system.

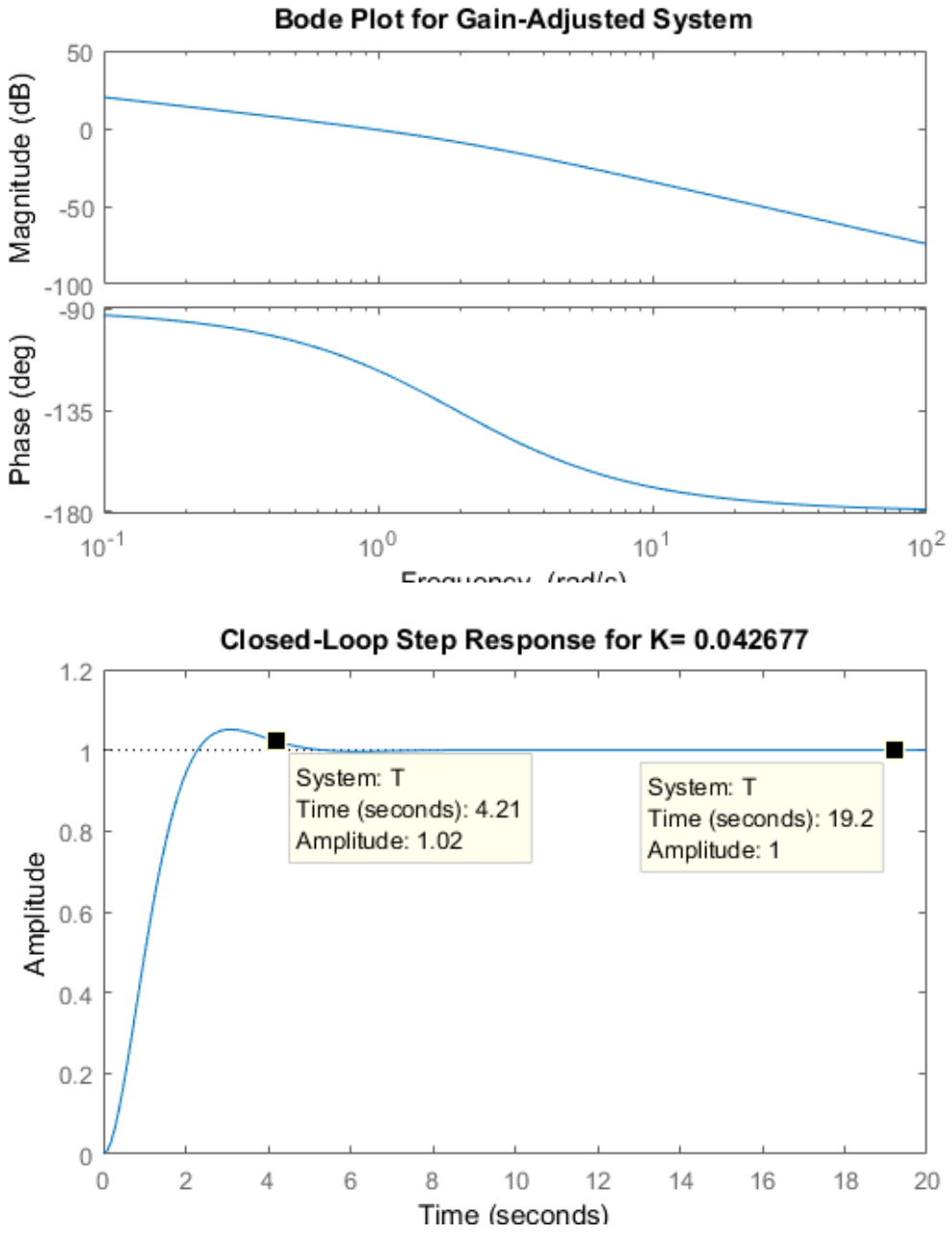

Figure 35: The system with gain adjustment.

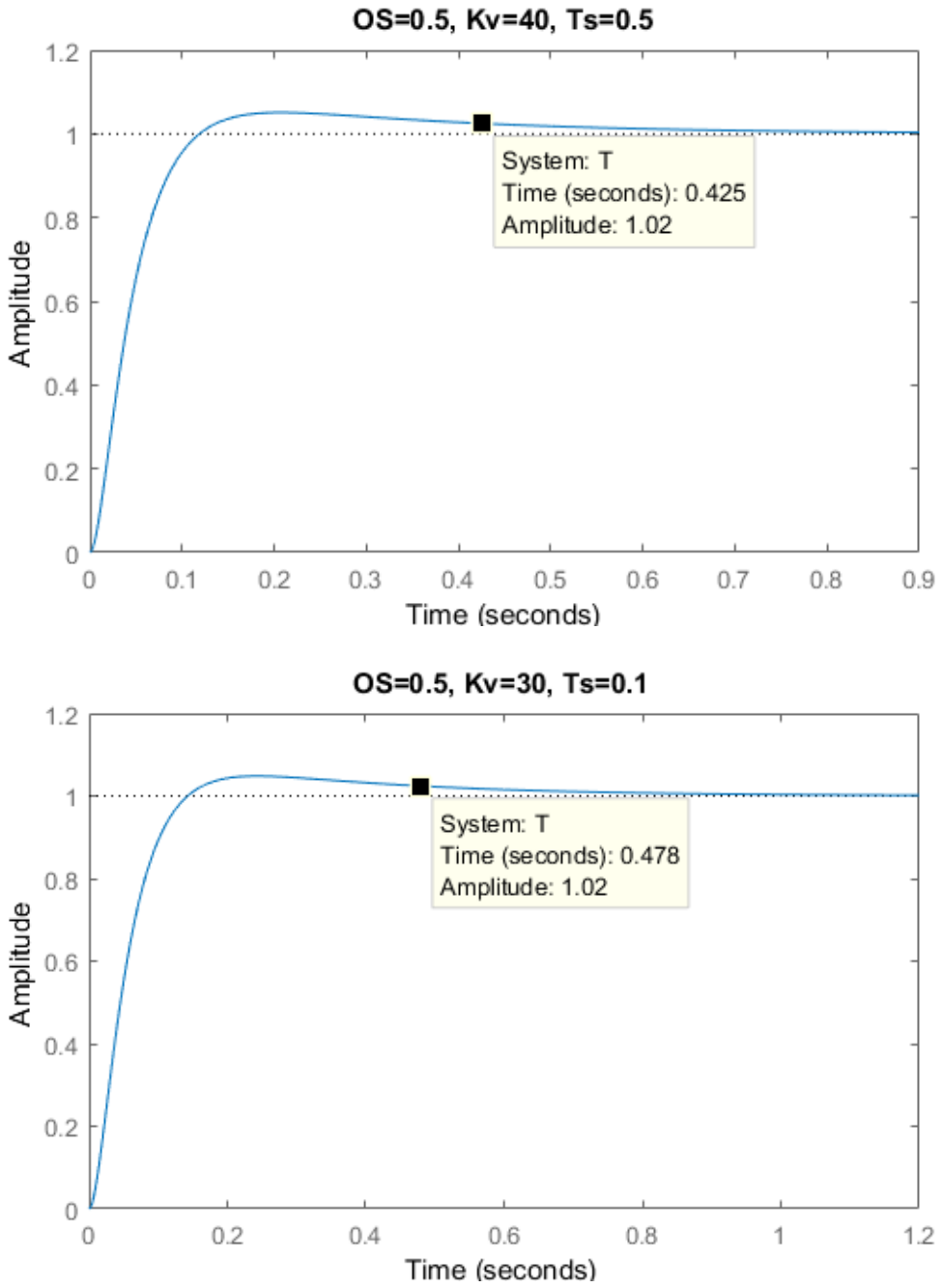

Figure 36: Two lead-controlled systems that satisfy the requirements, before the correction factor was changed.

B Lab 2

Unfortunately, higher quality images could not be produced due to the loss of original .m files. The result could not also be reproduced via the simulator block, because an error appears using the filtered derivative which can not be read due to read access on the simulator block.

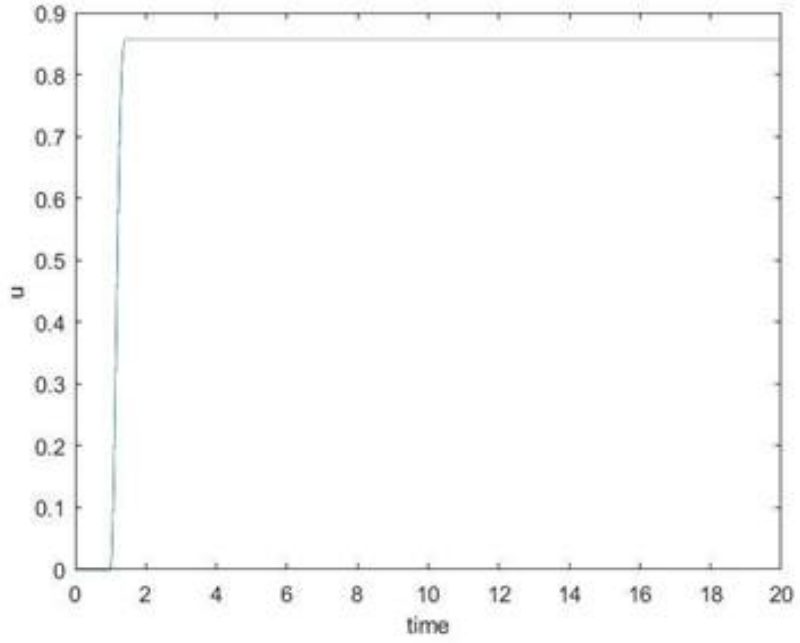

Figure 37: Step response beginning t=1s with proportional control.

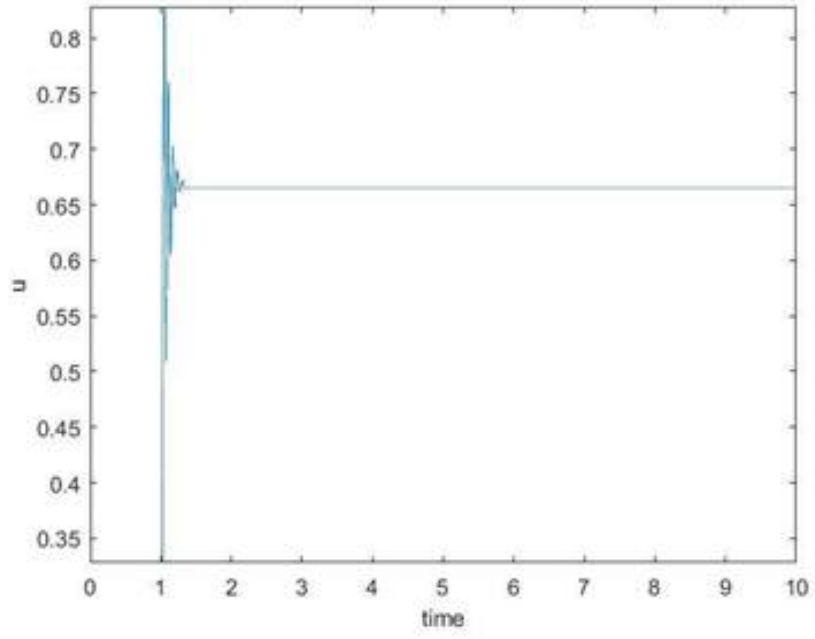

Figure 38: Step response beginning t=1s with derivative control.

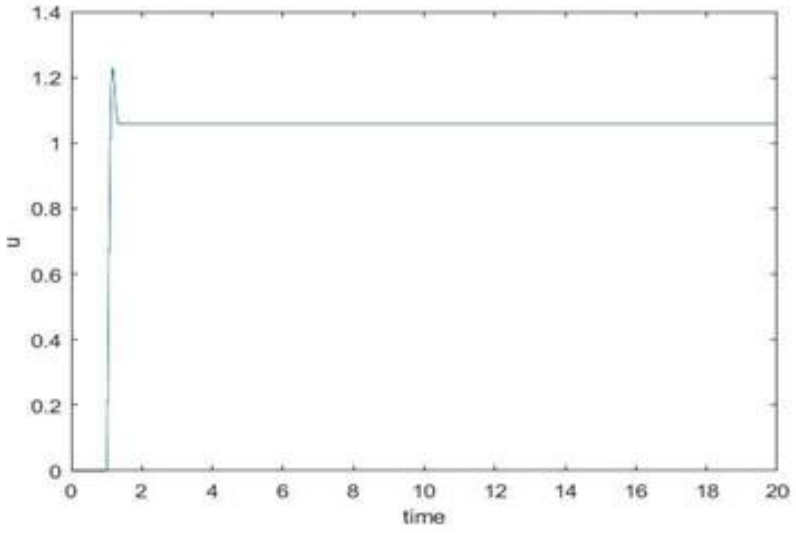

Figure 39: Step response beginning t=1s with PD control.

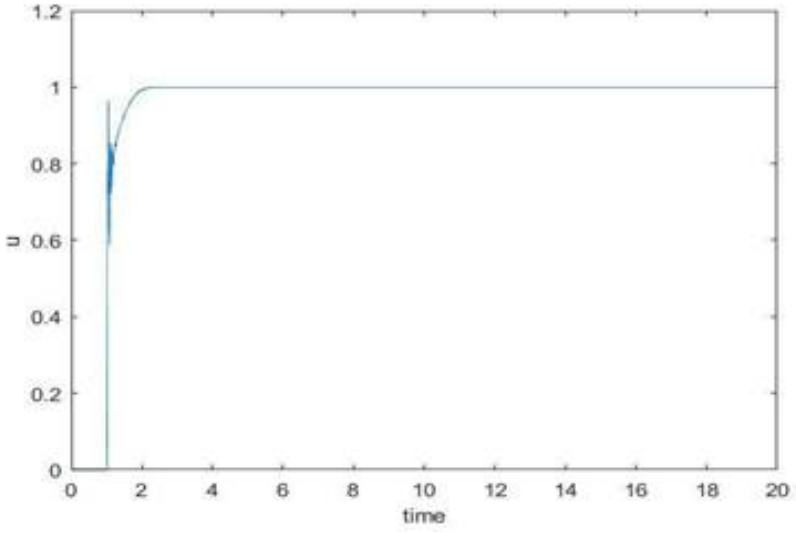

Figure 40: Step response beginning t=1s with PID control.

C Lab 3

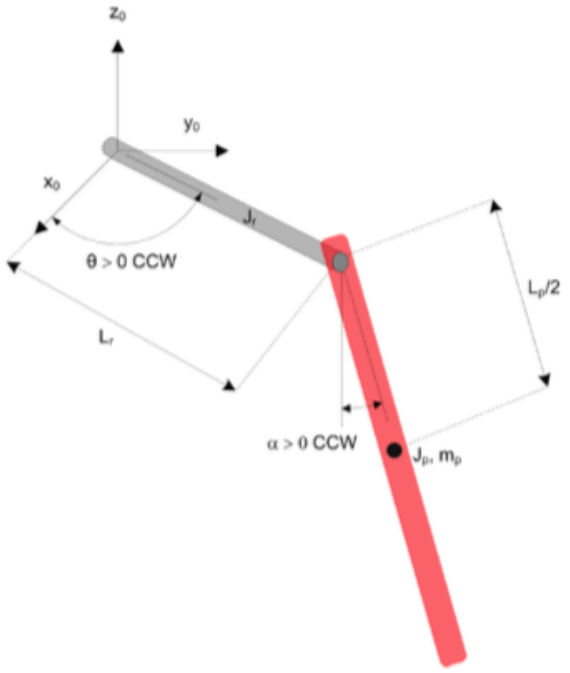

Parameter	Value	Unit
m_r	0.095	kg
m_p	0.024	kg
L_r	0.085	m
L_p	0.129	m
J_r	5.7×10^{-5}	kgm^2
J_p	1.8×10^{-4}	kgm^2
K_t	0.042	Nm/A
R_m	8.40	Ω
D_r	0.0015	Nms/rad
D_p	0.0005	Nms/rad

Figure 41: Left: The rotary pendulum model. Right: Given parameter values.

The system equations have been given as:

$$\ddot{\theta} = \frac{1}{J_T}\Big[-\Big(J_p + \frac{m_p L_p^2}{4}\Big)D_r\dot{\theta} + \frac{m_p L_p L_r D_p}{2}\dot{\alpha} + \frac{m_p^2 L_p^2 L_r g}{4}\alpha + \Big(J_p + \frac{m_p L_p^2}{4}\Big)\tau\Big] \quad (49)$$

$$\ddot{\alpha} = \frac{1}{J_T}\Big[\frac{m_p L_p L_r D_r}{2}\dot{\theta} - (J_r + m_p L_r^2)D_p\dot{\alpha} - \frac{m_p L_p g}{2}(J_r + m_p L_r^2)\alpha + \frac{m_p L_p L_r}{2}\tau \quad (50)$$

where $J_T = J_p m_p L_r^2 + J_r J_p + \frac{1}{4}J_r m_p L_p^2$ and $\tau = (K_t/R_m)u$.

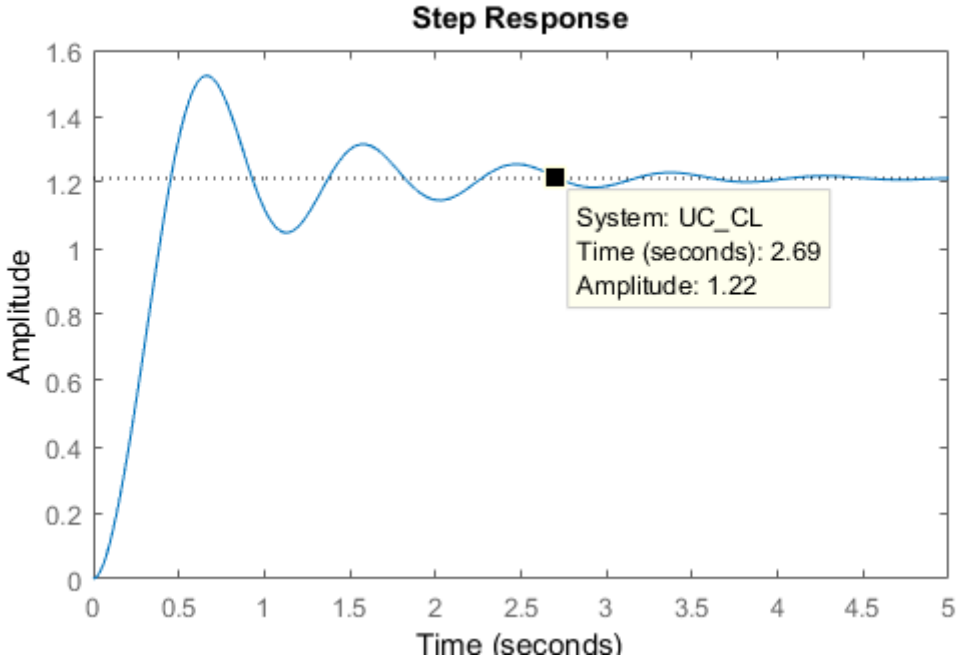

Figure 42: Open-loop step response for K=0.825 theoretically giving 5% OS.

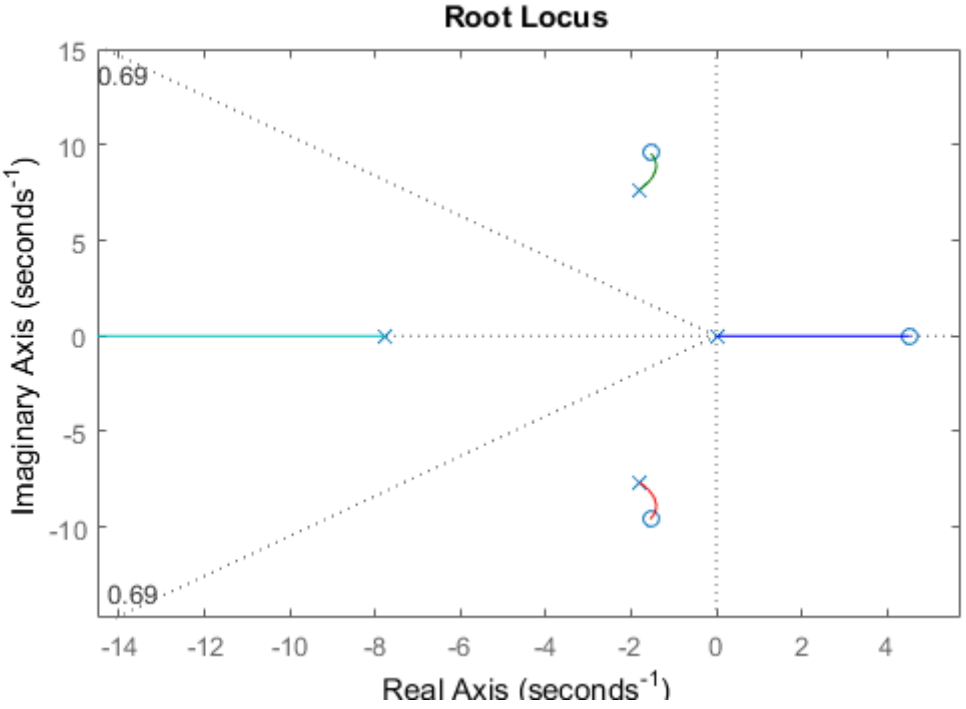

Figure 43: The root locus after addition of the compensator zero does not go through the 5% OS line.

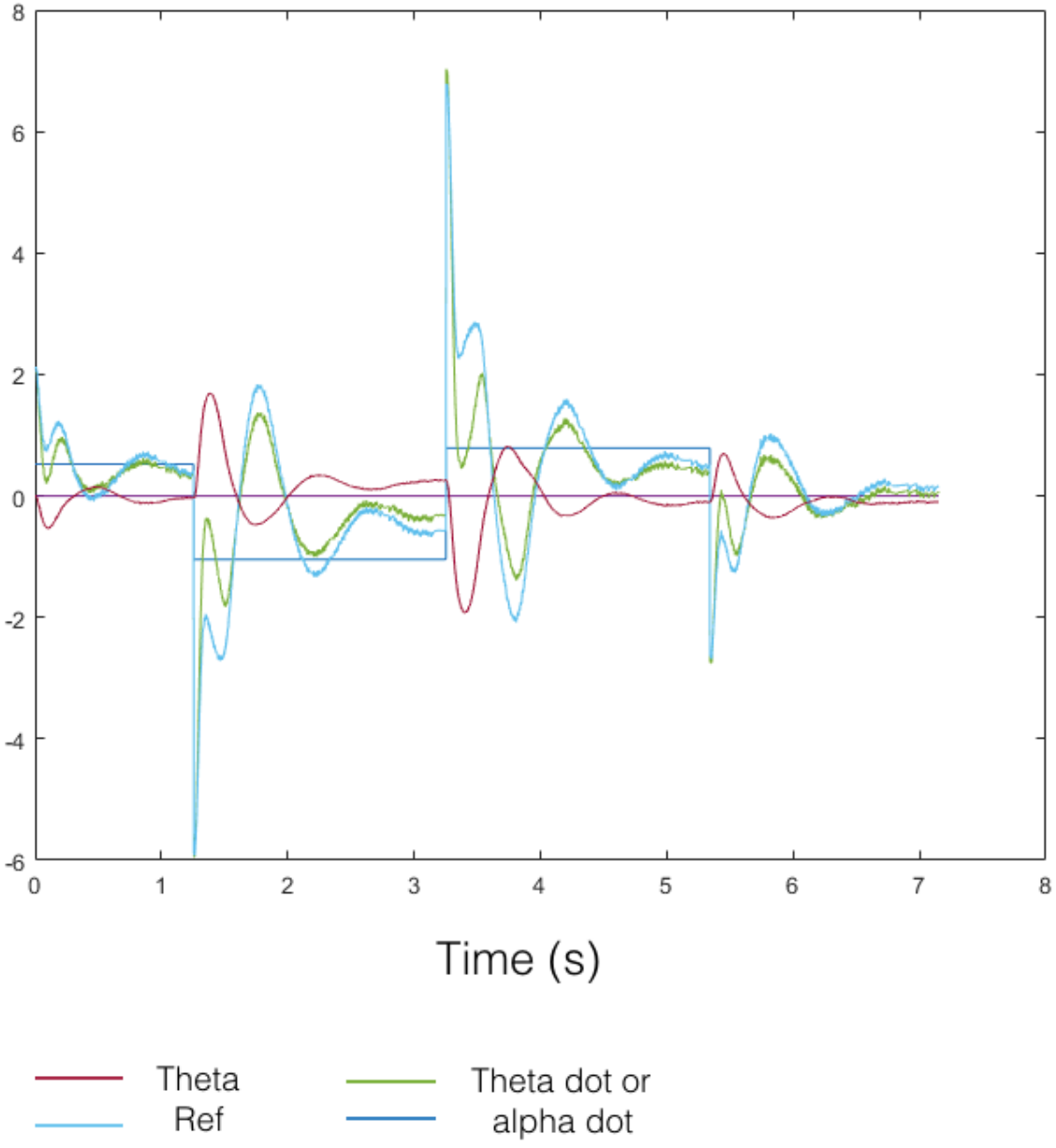

Figure 44: Outputs produced for the experiment performed during the laboratory.

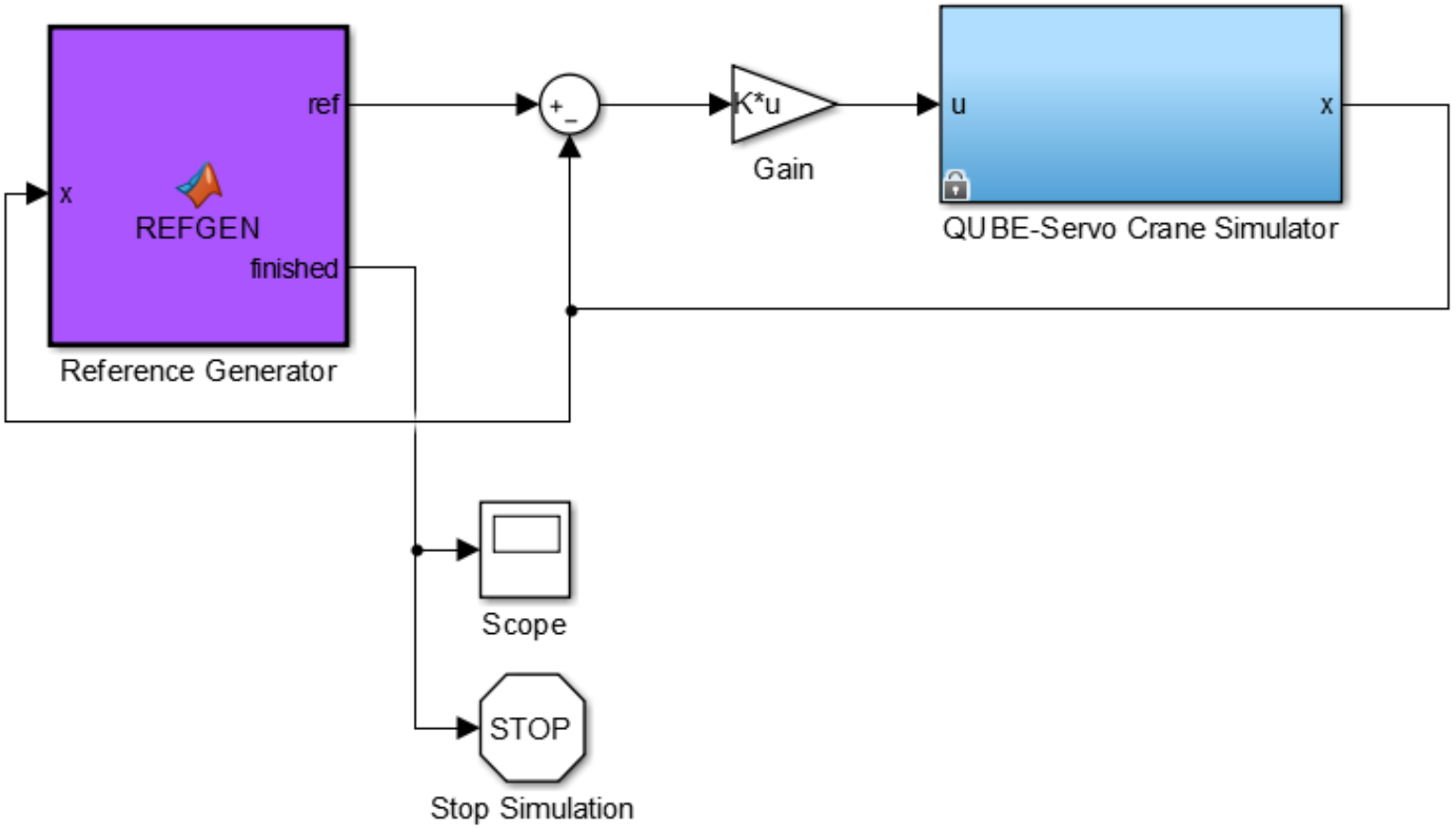

Figure 45: The Simulink model for the state-space controller.

```
m=5;
d=0.01;
k=10;
s=tf('s');
G=1/(m*s^2 + d*s + k);
bode(G);
hold on
k2 = 25;
G2=1/(m*s^2 + d*s + k2);
bode(G2);
```

```
%% PROPORTIONAL

clear all; close all; clc;

OS=5;           % [%]
zeta=(-log(OS/100))/(sqrt(pi^2+log(OS/100)^2));
PM=atan(2*zeta/(sqrt(-2*zeta^2+sqrt(1+4*zeta^4))))*(180/pi);
PA=-180+PM;

Iw = 0.52;      % [kgm^2]
Is = 0.4352;    % [kgm^2]
Kss = 20;       % [rad/V]
tau = 0.52;     % [s]
numerator = (Iw/Is)*(Kss/tau);
denominator = [1, 1/tau, 0];
G=tf(numerator,denominator);

w=0.01:0.01:1000;
[M,P]=bode(G,w);


for i=1:1:length(P);
    if P(i)-PA <= 0;
        M=M(i); % Current OL magnitude
        K=1/M;  % Required gain
        break
    end
end

T=feedback(K*G,1);
% step(T,20);
% title(['Closed-Loop Step Response for K= ',num2str(K)]);
% figure;
% bode(G);
% title('Bode Plot for Uncompensated System');
% figure;
% bode(K*G);
% title('Bode Plot for Gain-Adjusted System');
% figure; step(feedback(G,1),20);

% LAG

PM = PM + 20;   % Compensate for phase angle contribution of compensator
PA = -180+PM;

K=K*10;                             % Improve steady-state error tenfold
                                    % NB. Type 1 system - K is proportional to Kv

[M,P]=bode(K*G,w);

for j=1:1:length(P);
```

```
    if P(i)- PA <= 0;
        M=M(j);  % Current magnitude at phase angle
        wf=w(j); % Frequency at phase angle
        break
    end
end

wH=wf/10;                           % High frequency break of lag compensator (arbitrary)
wL=(wH/M);                          % Low frequency break of the lag compensator
num_c=[1 wH];
den_c=[1 wL];
Kc=wL/wH;                           % To yield Kv=1
Gc=tf(Kc*num_c,den_c);
GcG=Gc*G;
T=feedback(GcG,1);
step(T)
title('Closed-Loop Step Response for Lag-Compensated System')

s=tf('s');
sGcG=s*GcG;
sGcG=minreal(sGcG);                 % Cancel common terms
Kv=dcgain(sGcG);

%% LEAD

Kv = 30;
sG=s*G;
sG=minreal(sG);
K=dcgain(Kv/sG);
G=zpk(K*G);

Ts = 0.5;
wn=4/(zeta*Ts);
wBW=wn*sqrt((1-2*zeta^2)+sqrt(4*zeta^4-4*zeta^2+2)); % Required bandwidth

[M,P]=bode(G,w);
[Gm,Pm,Wcg,Wcp]=margin(G);

Pc = PM - Pm;                       % Required phase contribution

beta=(1-sin(Pc*pi/180))/(1+sin(Pc*pi/180));
Mc=1/sqrt(beta);                    % Compensator magnitude at peak of phase curve

for k=1:1:length(M);
    if M(k)-(1/Mc)<=0;
        wmax=w(k);                  % New phase margin frequency
        break
    end
end

wL=wmax*sqrt(beta);                 % Low frequency break of lead compensator
```

```
wH=wL/beta;                             % High frequency break of lead compensator
Kc=1/beta;                              % Gain of lead compensator

Gc=tf(Kc*[1 wL],[1 wH]);
Gc=zpk(Gc);

Ge=G*Gc;
T=feedback(Ge,1);
step(T);
title('Correction Factor-Adjusted: OS=5, Ts= 0.5, Kv=30');

sGe=s*Ge;
sGe=minreal(sGe);
Kv=dcgain(sGe);
```

```
clc;

s = tf('s');

wn = 0.2; % [rad/s]
m = 10; % [kg]
Js = 0.4352; % [kg.m^2]
Jp = 9.083; % [kg.m^2]
k = wn^2*Jp; % [Nm]
d = 1*10^-3; % [Ns/m]

G = (Jp*s^2 + d*s + k)/(Js*Jp*s^4 + d*(Jp+Js)*s^3 + k*(Jp+Js)*s^2);
G = minreal(G);
% rlocus(G);
% [z, p, k] = zpkdata(G);
% syms s
% collect(tf2,s)

A = [0 1 0 0; -k/Js -d/Js k/Js d/Js; 0 0 0 1; k/Jp d/Jp -k/Jp -d/Jp];
B = [0; 1; 0; 0];
C = [1 0 0 0];

sys = ss(A,B,C,0);
% bode(sys);
sys_order = order(sys); % 4th order
c_det = det(ctrb(A,B)); % Non-zero determinant -> Controllable
o_det = det(obsv(A,C)); % Non-zero determinant -> Observable
z = zero(sys);
p = eig(A);

OS = 0.1; % [%]
zeta = -log(OS/100)/sqrt(pi^2 + log(OS/100)^2);
phi = acosd(zeta); % [deg]
T_s = 2.6; % [s]

% Desired dominant pole locations
sigma = pi/(T_s);
omega_d = sigma*tand(phi);

i = sqrt(-1);
p1 = -sigma + omega_d*i;
p2 = -sigma - omega_d*i;
p3 = -0.0001 + 0.2i; % To cancel zeros
p4 = -0.0001 - 0.2i; % To cancel zeros

K = place(A,B,[p1 p2 p3 p4]);
sys_cl = ss(A-B*K,B,C,0);
SS_error = 1+C*(A-B*K)^-1*B;
% step(sys_cl,3);

% Add integral control
```

```
Aa = [0 1 0 0 0;
    -k/Js -d/Js k/Js d/Js 0;
    0 0 0 1 0;
    k/Jp d/Jp -k/Jp -d/Jp 0;
    1 0 0 0 0];
Ba = [0; 1; 0; 0; 0];
Br = [0 ; 0 ; 0; 0; -1];
Ca = [1 0 0 0 0];

p5 = -10;
Ka = place(Aa,Ba,[p1,p2,p3,p4,p5]);

sys_cl_integral = ss(Aa-Ba*Ka,Br,Ca,0);
% step(sys_cl_integral);

% t=0:0.001:10;
% u = ones(size(t));
% x0 = [0 0 0 0 0];
% [yOut, tOut, xOut ]=lsim(sys_cl_integral,u,t,x0);
% figure; plot(t,yOut);
% torque = -Ka*xOut';
% figure; plot(t,torque)
% xlabel('Time (s)');
% ylabel('Torque (Nm)');


%% Q2.3

settling_time = 3.39;
ramp_seconds = ceil(settling_time);
M_size = 46*ramp_seconds;
u = ones(1,M_size);
amplitude = 1;

time_divisions = 2;
no_to_fill = ramp_seconds*time_divisions;
 for a = 1:46
     for j=1:no_to_fill
        u(1,(no_to_fill*a)-no_to_fill+j)=amplitude;
     end
     amplitude=amplitude+1;
 end

t=0:(1/time_divisions):(length(u)-1)/2;
x0 = [0 0 0 0 0];
[yOut, tOut, xOut ]=lsim(sys_cl_integral,u,t,x0);
figure; plot(t,yOut);
xlabel('Time (s)');
ylabel('Satellite position (deg)');
torque = -Ka*xOut';
```

```
figure; plot(t,torque)
xlabel('Time (s)');
ylabel('Torque (Nm)');
figure; plot(t,u);
xlabel('Time (s)');
ylabel('Reference (deg)');
```

```
m_s = 0.65;
m_r = 0.42;
m_p = 10;
m_f = 100;
M_T = m_s + m_r + 2*m_p + m_f;

t = x_out.time;
x = x_out.signals.values;
v = v_out.signals.values;
a = a_out.signals.values;
m = m_out.signals.values;

plot(t,x,t,v,t,a);

F = 24;
```

```
%% Root Locus Method for Lab 3 Crane Control

pmr = 0.095;
mp = 0.024;
Lr = 0.085;
Lp = 0.129;
Jr = 5.7*10^-5;
Jp = 1.8*10^-4;
Kt = 0.042;
Rm = 8.4;
Dr = 0.0015;
Dp = 0.0005;
g = 9.81;

tau_coef = Kt/Rm;
JT = Jp*mp*Lr^2 + Jr*Jp + 0.25*Jr*mp*Lp^2;

A = -(Jp+0.25*mp*Lp^2)*Dr/JT;
B = 0.5*mp*Lp*Lr*Dp/JT;
C = 0.25*mp^2*Lp^2*Lr*g/JT;
D = tau_coef*(Jp + 0.25*mp*Lp^2)/JT;

E = 0.5*mp*Lp*Lr*Dr/JT;
F = -(Jr+mp*Lr^2)*Dp/JT;
G = -0.5*mp*Lp*g*(Jr+mp*Lr^2)/JT;
H = 0.5*mp*Lp*Lr*tau_coef/JT;

s = tf('s');
UC_OL = (D*s^2 + (B*H-D*F)*s + C*H - D*G)/(s^4 - (F+A)*s^3 - (G-A*F+B*E)*s^2 + (A*G-C*E)↙
*s);
% step(UC_OL); % Ramp response
% step(feedback(UC_OL,1)); % Settling time of 4.11s when K=1


%% DESIGN FOR OVERSHOOT

OS = 5; % [%]
zeta = -log(OS/100)/sqrt(pi^2 + log(OS/100)^2);
phi = acosd(zeta); % [deg]

% rlocus(UC_OL);
% sgrid(zeta,0);

% Current dominant pole location
sigma = 4.68;
omega_d = 4.91;
T_s = 4/sigma;
K = 0.825;
UC_CL = feedback(UC_OL,K);
% step(UC_CL); % Settling time of 2.69s for K at operating point
```

```
% OL Poles & Zeros
P1 = 7.72;
P2 = 0;
P3_R = 1.79;
P3_I = 7.67;
Z1_R = 1.55;
Z1_I = 9.58;

%% SETTLING TIME

% Desired dominant pole location
sigma = pi/(0.5*T_s); % 7.3513
omega_d = sigma*tand(phi); % 7.7093

% Angle contribution
theta_P1 = atand(omega_d/(P1-sigma));
theta_P2 = 180 - atand(omega_d/sigma);
theta_P3 = 180 - atand((omega_d-P3_I)/(sigma-P3_R));
theta_P3_conj = 180 - atand((sigma-P3_R)/(P3_I + omega_d));
theta_Z1 = 270 - atand((Z1_I-omega_d)/(sigma-Z1_R));
theta_Z1_conj = 180 - atand((sigma-Z1_R)/(Z1_I + omega_d));

%% Compensating D zero
theta_Z =  theta_P1 + theta_P2 + theta_P3 - theta_Z1 + theta_P3_conj - theta_Z1_conj +↙
180;
Z = (omega_d/tand(theta_Z)) + sigma;

PD = (s+Z)*UC_OL;
rlocus(PD);
sgrid(zeta,0);
```

```
clc; clear all;

pmr = 0.095;
mp = 0.024;
Lr = 0.085;
Lp = 0.129;
Jr = 5.7*10^-5;
Jp = 1.8*10^-4;
Kt = 0.042;
Rm = 8.4;
Dr = 0.0015;
Dp = 0.0005;
g = 9.81;

tau_coef = Kt/Rm;
JT = Jp*mp*Lr^2 + Jr*Jp + 0.25*Jr*mp*Lp^2;

A_coef = -(Jp+0.25*mp*Lp^2)*Dr/JT;
B_coef = 0.5*mp*Lp*Lr*Dp/JT;
C_coef = 0.25*mp^2*Lp^2*Lr*g/JT;
D = tau_coef*(Jp + 0.25*mp*Lp^2)/JT;

E = 0.5*mp*Lp*Lr*Dr/JT;
F = -(Jr+mp*Lr^2)*Dp/JT;
G = -0.5*mp*Lp*g*(Jr+mp*Lr^2)/JT;
H = 0.5*mp*Lp*Lr*tau_coef/JT;

s = tf('s');
theta_on_U = (D*s^2 + (B_coef*H-D*F)*s + C_coef*H - D*G)/(s^4 - (F+A_coef)*s^3 - (G-↙
A_coef*F+B_coef*E)*s^2 + (A_coef*G-C_coef*E)*s);
[z1, poles1, k1] = zpkdata(theta_on_U);  % All poles on LHS half-plane -> Stable
denom = s^2-F*s-G;
denom2 = denom*(s^2-A_coef*s);
alpha_on_U = ((D*E*s/denom2) + H/denom)/...
    (1-(E*s*(B_coef*s+C_coef))/denom2);
alpha_on_U = minreal(alpha_on_U); % All poles on LHS half-plane -> Stable
[z2, poles2, k2] = zpkdata(alpha_on_U);

%% State Space Matrices

A = [0 0 1 0; 0 0 0 1; 0 C_coef A_coef B_coef; 0 G E F];
B = [0; 0; D; H];
C = [1 0 0 0];

c_rank = rank(ctrb(A,B)); % Full rank
c_det = det(ctrb(A,B)); % Non-zero determinant -> Controllable
o_rank = rank(obsv(A,C)); % Full rank
o_det = det(obsv(A,C)); % Non-zero determinant -> Observable

OS = 1; % [%]
zeta = -log(OS/100)/sqrt(pi^2 + log(OS/100)^2);
```

```
phi = acosd(zeta); % [deg]
T_s = 0.7; % [s]
% Desired dominant pole locations
sigma = pi/(T_s);
omega_d = sigma*tand(phi);

i = sqrt(-1);
p1 = -sigma + omega_d*i;
p2 = -sigma - omega_d*i;
p3 = -1.54923272843930 + 9.57631072896759i; % To cancel zeros
p4 = -1.54923272843930 - 9.57631072896759i; % To cancel zeros

sys = ss(A,B,C,0);

K = place(A,B,[p1 p2 p3 p4]);
sys_cl = ss(A-B*K,B,C,0);
step(sys_cl);

SS_error = 1+C*(A-B*K)^-1*B;
```